REPORT No. 906

DETERMINATION OF STRESSES IN GAS-TURBINE DISKS SUBJECTED TO PLASTIC FLOW AND CREEP

By M. B. MILLENSON and S. S. MANSON

SUMMARY

A finite-difference method previously presented for computing elastic stresses in rotating disks is extended to include the computation of the disk stresses when plastic flow and creep are considered. A finite-difference method is employed to eliminate numerical integration and to permit nontechnical personnel to make the calculations with a minimum of engineering supervision. Illustrative examples are included to facilitate explanation of the procedure by carrying out the computations on a typical gas-turbine disk through a complete running cycle.

The results of the numerical examples presented indicate that plastic flow markedly alters the elastic-stress distribution.

INTRODUCTION

With the advent of jet propulsion as a motive force for aircraft, the gas turbine has become an important source of power. In most machinery, design stresses are limited by the yield strength or the creep strength of the material employed, together with a certain factor of safety, and little or no analytical consideration is given to the occurrence of plastic flow under operating conditions. Gas-turbine disks, however, are required to operate under thermal gradients and centrifugal forces producing stresses that, in materials currently available, frequently exceed the yield strength, resulting in plastic flow. The interaction of plastic flow and creep, together with the variation of thermal gradients through a series of cycles consisting in starting, running, and stopping, can produce stress distributions and even failures that might not be anticipated on a basis of elastic-stress analysis.

A rapid routine method of elastic-stress analysis of rotating disks is presented in reference 1, which gives accurate values of the true stresses in disks provided that the yield strength of the material is not exceeded. The finite-difference method of reference 1 has been extended at the NACA Cleveland laboratory to include consideration of plastic flow and creep, which thus allows calculation of the true stresses in a gas-turbine disk and gives the variation of stress distribution with time. The handling of plastic flow is somewhat less routine than the calculation of the elastic stresses in that a repetitive trial procedure is required. With practice, the correct value can be obtained on the fourth or fifth trial. The computation of the effect of creep, although in procedure the same as the computation of plastic flow, is a direct calcu-

lation requiring no trial-and-error procedures. Because the method eliminates numerical integration, nontechnical personnel can make the calculations with a minimum of engineering supervision.

SYMBOLS

The following symbols are used:

c creep rate under stress σ_e, (in./(in.)(hr))
E elastic modulus of disk material, (lb/sq in.)
h axial thickness of disk, (in.)
R ratio $\left(\dfrac{3\epsilon_p}{2\sigma_e}\right)$
r radial distance, (in.)
T temperature, (°F)
u radial displacement, (in.)
α coefficient of thermal expansion between actual temperature and temperature at zero thermal stress, (in./(in.)(°F))
Γ total creep under stress σ_e, (in./in.)
Δ plastic increment of strain, (in./in.)
Δ_r plastic increment of strain in radial direction, (in./in.)
Δ_t plastic increment of strain in tangential direction, (in./in.)
ΔT temperature increment above temperature of zero thermal stress, (°F)
δ_r creep increment in radial direction, (in./in.)
δ_t creep increment in tangential direction, (in./in.)
ϵ strain, (in./in.)
ϵ_p plastic strain corresponding to stress σ_e in tensile specimen, (in./in.)
ϵ_r radial strain, (in./in.)
ϵ_t tangential strain, (in./in.)
μ Poisson's ratio
ρ mass density of disk material, ((lb)(sec^2)/in.^{4})
σ stress, (lb/sq in.)
σ_e equivalent tensile stress, (lb/sq in.)
σ_r radial stress, (lb/sq in.)
σ_t tangential stress, (lb/sq in.)
σ_y proportional elastic limit, (lb/sq in.)
τ time during which creep occurs, (hr)
ω angular velocity, (radians/sec)

The following supplementary subscripts are used for denoting values of the preceding symbols in connection with the finite-difference solution:

n nth point station

$n-1$ $(n-1)$st point station

a station at smallest disk radius considered
(For disk with a central hole, this station is taken at the radius of the central hole; for a solid disk, this station is taken at a radius approximately 5 percent of the rim radius.)

b station at rim of disk or base of blades

The following supplementary symbols denote combinations of the foregoing symbols:

$\left.\begin{array}{c} A_{r,n} \\ A_{t,n} \\ B_{r,n} \\ B_{t,n} \end{array}\right\}$ stress coefficients defined by equations $\sigma_{r,n}=A_{r,n}\sigma_{t,a}+B_{r,n}$ $\sigma_{t,n}=A_{t,n}\sigma_{t,a}+B_{t,n}$

$C_n = r_n h_n$

$C'_n = \dfrac{\mu_n}{E_n} + \dfrac{(1+\mu_n)(r_n-r_{n-1})}{2E_n r_n}$

$D_n = \dfrac{1}{2}(r_n-r_{n-1})h_n$

$D'_n = \dfrac{1}{E_n} + \dfrac{(1+\mu_n)(r_n-r_{n-1})}{2E_n r_n}$

$F_n = r_{n-1}h_{n-1}$

$F'_n = \dfrac{\mu_{n-1}}{E_{n-1}} - \dfrac{(1+\mu_{n-1})(r_n-r_{n-1})}{2E_{n-1}r_{n-1}}$

$G_n = \dfrac{1}{2}(r_n-r_{n-1})h_{n-1}$

$G'_n = \dfrac{1}{E_{n-1}} - \dfrac{(1+\mu_{n-1})(r_n-r_{n-1})}{2E_{n-1}r_{n-1}}$

$H_n = \dfrac{1}{2}\omega^2(r_n-r_{n-1})(\rho_n h_n r_n^2 + \rho_{n-1}h_{n-1}r_{n-1}^2)$

$H'_n = \alpha_n \Delta T_n - \alpha_{n-1}\Delta T_{n-1}$

$K_n = \dfrac{F'_n D_n - F_n D'_n}{C'_n D_n - C_n D'_n}$

$K'_n = \dfrac{C_n F'_n - C'_n F_n}{C'_n D_n - C_n D'_n}$

$L_n = -\dfrac{G'_n D_n + G_n D'_n}{C'_n D_n - C_n D'_n}$

$L'_n = -\dfrac{C'_n G_n + C_n G'_n}{C'_n D_n - C_n D'_n}$

$M_n = \dfrac{D'_n H_n + D_n(H'_n - P'_n - Q'_n)}{C'_n D_n - C_n D'_n}$

$M'_n = \dfrac{C'_n H_n + C_n(H'_n - P'_n - Q'_n)}{C'_n D_n - C_n D'_n}$

(M_n and M'_n are defined in reference 1 for the special case $P'_n = Q'_n = 0$)

$P'_n = \Delta_{r,n}\left(\dfrac{r_n-r_{n-1}}{2r_n}\right) + \Delta_{r,n-1}\left(\dfrac{r_n-r_{n-1}}{2r_{n-1}}\right) - \Delta_{t,n}\left(1+\dfrac{r_n-r_{n-1}}{2r_n}\right) +$
$\qquad \Delta_{t,n-1}\left(1-\dfrac{r_n-r_{n-1}}{2r_{n-1}}\right)$

$Q'_n = \delta_{r,n}\left(\dfrac{r_n-r_{n-1}}{2r_n}\right) + \delta_{r,n-1}\left(\dfrac{r_n-r_{n-1}}{2r_{n-1}}\right) - \delta_{t,n}\left(1+\dfrac{r_n-r_{n-1}}{2r_n}\right) +$
$\qquad \delta_{t,n-1}\left(1-\dfrac{r_n-r_{n-1}}{2r_{n-1}}\right)$

ANALYSIS OF PLASTIC FLOW AND CREEP

Assumptions.—Four assumptions are made in the subsequent analysis:

1. The disk material is linearly elastic up to a limiting stress value, called the proportional elastic limit, and above this limit plastic flow occurs.

2. All variables of material properties and operating conditions are symmetrical about the axis of rotation.

3. Axial stresses may be neglected and the radial and tangential stresses are uniform across the thickness of the disk.

4. Temperatures are uniform across the thickness of the disk.

Outline of method.—In any thin rotating disk, the complete stress state is defined when the two principal stresses, radial σ_r and tangential σ_t, are known at every radius. Two equations relating these stresses to the radius are required to specify the stress distribution. The first of these equations can be determined from the conditions of equilibrium of an element of the disk and involves no elastic properties of the material. The second is derived from the compatibility conditions, which state the interrelation of radial and tangential strains. The compatibility conditions are dependent upon stress-strain phenomena and must therefore include any departure from linear elasticity. When modification to allow for any possible departure from Hooke's law is made, the compatibility conditions become true for any value of stress. The equation derived from the compatibility conditions thus modified, together with the equilibrium equation, is treated by the finite-difference method of reference 1, and similar equations are obtained. These equations result in additional terms in the final equations, which are used to modify the result of the elastic calculation.

Whenever stresses under discussion have been calculated by the method of reference 1 only, they will be referred to as "elastic stresses"; where plastic flow and creep have been taken into account, the stresses will be referred to as "plastic stresses."

Derivation of method.—The equilibrium equation, which applies to both the elastic and plastic conditions, is

$$\frac{d}{dr}(rh\sigma_r) - h\sigma_t + \rho\omega^2 r^2 h = 0 \qquad (1)$$

The elastic compatibility relations given in terms of the radial displacement are

$$\epsilon_r = \frac{du}{dr} = \frac{\sigma_r - \mu\sigma_t}{E} + \alpha\Delta T \qquad (2)$$

and

$$\epsilon_t = \frac{u}{r} = \frac{\sigma_t - \mu\sigma_r}{E} + \alpha\Delta T \qquad (3)$$

Equations (2) and (3) must be modified to include consideration of plastic flow. When a material is stressed beyond the proportional elastic limit, the strain in the material is different from that indicated by Hooke's law. The strain under such a load may be considered as being made up of two components, one elastic as predicted by the laws of elasticity and one an increment of strain due to the flow that occurs. Rewriting equations (2) and (3) on this basis gives

$$\epsilon_r = \frac{du}{dr} = \frac{\sigma_r - \mu \sigma_t}{E} + \alpha \Delta T + \Delta_r \qquad (4)$$

$$\epsilon_t = \frac{u}{r} = \frac{\sigma_t - \mu \sigma_r}{E} + \alpha \Delta T + \Delta_t \qquad (5)$$

Similarly, any creep that occurs represents an additional departure from elastic behavior, which further modifies equations (2) and (3) to

$$\epsilon_r = \frac{du}{dr} = \frac{\sigma_r - \mu \sigma_t}{E} + \alpha \Delta T + \Delta_r + \delta_r \qquad (6)$$

$$\epsilon_t = \frac{u}{r} = \frac{\sigma_t - \mu \sigma_r}{E} + \alpha \Delta T + \Delta_t + \delta_t \qquad (7)$$

When the parameter u is eliminated as in reference 1,

$$\frac{d}{dr}\left(\frac{1}{E}\sigma_t - \frac{\mu}{E}\sigma_r + \alpha \Delta T + \Delta_t + \delta_t\right) = \frac{1+\mu}{Er}(\sigma_r - \sigma_t) + \frac{\Delta_r - \Delta_t}{r} + \frac{\delta_r - \delta_t}{r} \qquad (8)$$

Applying the finite-difference method to equations (1) and (8) and using the notation introduced in the section Symbols gives

$$C_n \sigma_{r,n} - D_n \sigma_{t,n} = F_n \sigma_{r,n-1} + G_n \sigma_{t,n-1} - H_n \qquad (9)$$

and

$$C'_n \sigma_{r,n} - D'_n \sigma_{t,n} = F'_n \sigma_{r,n-1} - G'_n \sigma_{t,n-1} + H'_n - P'_n - Q'_n \qquad (10)$$

The solution of the equations is facilitated by the substitution of the stress coefficients $A_{r,n}$, $A_{t,n}$, $B_{r,n}$, and $B_{t,n}$ into equations (9) and (10). Proceeding as in reference 1 results in the equations

$$\left.\begin{aligned} C_n A_{r,n} - D_n A_{t,n} - F_n A_{r,n-1} - G_n A_{t,n-1} = 0 \\ C'_n A_{r,n} - D'_n A_{t,n} - F'_n A_{r,n-1} + G'_n A_{t,n-1} = 0 \\ C_n B_{r,n} - D_n B_{t,n} - F_n B_{r,n-1} - G_n B_{t,n-1} + H_n = 0 \\ C'_n B_{r,n} - D'_n B_{t,n} - F'_n B_{r,n-1} + \\ G'_n B_{t,n-1} - H'_n + P'_n + Q'_n = 0 \end{aligned}\right\} \qquad (11)$$

All but the last of equations (11) and equations (15) of reference 1 are identical. When equations (11) are solved for $A_{r,n}, A_{t,n}, B_{r,n},$ and $B_{t,n}$,

$$\left.\begin{aligned} A_{r,n} = K_n A_{r,n-1} + L_n A_{t,n-1} \\ A_{t,n} = K'_n A_{r,n-1} + L'_n A_{t,n-1} \\ B_{r,n} = K_n B_{r,n-1} + L_n B_{t,n-1} + M_n \\ B_{t,n} = K'_n B_{r,n-1} + L'_n B_{t,n-1} + M'_n \end{aligned}\right\} \qquad (12)$$

The symbols K_n, K'_n, L_n, and L'_n have the same meaning as in reference 1. The M_n and M'_n terms are now defined as

$$M_n = \frac{D'_n H_n + D_n(H'_n - P'_n - Q'_n)}{C'_n D_n - C_n D'_n} \qquad (13)$$

$$M'_n = \frac{C'_n H_n + C_n(H'_n - P'_n - Q'_n)}{C'_n D_n - C_n D'_n} \qquad (13a)$$

The elastic case of reference 1 thus becomes a special case of the more general problem in which P'_n and Q'_n are both zero.

Evaluation of plastic terms. —In order to apply the finite-difference method to problems involving plastic flow, a relation between stresses and strains in the plastic region must be established. In reference 2, a numerical-integration method for computing disk stresses is presented in which elongation is assumed to proceed at constant stress when the proportional limit is reached. References 3 and 4 present equations for the plastic relation of stress to strain based on the maximum distortion theory. Relations can be derived from the equations given in reference 4, which form a convenient means of finding the plastic increments corresponding to the stresses present in the disk. Rewriting these equations in the notation of this report and letting the subscripts 1, 2, and 3 denote the three principal directions in the most general case give

$$\left.\begin{aligned} \Delta_1 = \frac{R}{3}\left[(\sigma_1 - \sigma_2) + (\sigma_1 - \sigma_3)\right] \\ \Delta_2 = \frac{R}{3}\left[(\sigma_2 - \sigma_1) + (\sigma_2 - \sigma_3)\right] \\ \Delta_3 = \frac{R}{3}\left[(\sigma_3 - \sigma_1) + (\sigma_3 - \sigma_2)\right] \end{aligned}\right\} \qquad (14)$$

$$\sigma_e = \frac{1}{\sqrt{2}}\sqrt{(\sigma_1 - \sigma_2)^2 + (\sigma_2 - \sigma_3)^2 + (\sigma_3 - \sigma_1)^2} \qquad (15)$$

where the ratio R is defined in terms of the corresponding uniaxial stress σ_e and plastic strain ϵ_p in a tensile specimen by the relation

$$R = \frac{3\epsilon_p}{2\sigma_e} \qquad (16)$$

When equations (14), (15), and (16) are reduced to the biaxial condition, which is assumed to prevail in the disk (that is, $\sigma_3 = 0$), and the finite-difference notation is introduced

$$\left.\begin{aligned} \Delta_{r,n} = \frac{R}{3}(\sigma_{r,n} - \sigma_{t,n} + \sigma_{r,n}) \\ \Delta_{t,n} = \frac{R}{3}(\sigma_{t,n} - \sigma_{r,n} + \sigma_{t,n}) \end{aligned}\right\} \qquad (17)$$

$$\sigma_{e,n} = \sqrt{\sigma_{r,n}^2 - \sigma_{r,n}\sigma_{t,n} + \sigma_{t,n}^2} \qquad (18)$$

and

$$R = \frac{3\epsilon_{p,n}}{2\sigma_{e,n}} \qquad (19)$$

FIGURE 1.—Uniaxial stress-strain curve showing relation between stress $\sigma_{e,n}$ and plastic strain $\epsilon_{p,n}$.
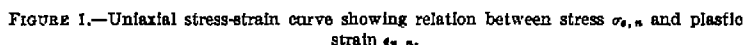
Substituting equation (19) into equations (17) gives

$$\left.\begin{aligned}\Delta_{r,n}&=\frac{\epsilon_{p,n}}{2\sigma_{e,n}}\left(2\sigma_{r,n}-\sigma_{t,n}\right)\\\Delta_{t,n}&=\frac{\epsilon_{p,n}}{2\sigma_{e,n}}\left(2\sigma_{t,n}-\sigma_{r,n}\right)\end{aligned}\right\}\qquad(20)$$

A typical uniaxial stress-strain curve illustrating the relation between effective stress $\sigma_{e,n}$ and effective plastic strain $\epsilon_{p,n}$ on such a curve is shown in figure 1. Investigations at the National Physical Laboratory of Great Britain on turbine-disk alloys and experiments by Taylor and Quinney (reference 5) were found to correlate well with equations (20) for the range of strains over which the volume of the material is approximately constant.

Equations (20) give the relations between plastic strains and true stresses that will be used as the basis for numerical calculations in the present report. The method of stress analysis to be presented does not depend, however, on the validity of these equations. As more accurate relations are determined between stresses and strains, these relations may readily be used in place of equations (20).

Calculation of plastic flow when no previous plastic flow has occurred.—The determination of the plastic stresses in the disk resolves itself into the problem of finding corre-

sponding stresses and strains that satisfy equilibrium and compatibility equations (9) and (10), and biaxial stress-strain equations (20). The problem is approached by first computing the elastic stresses, and the equivalent uniaxial tensile stress at each station is determined from equation (18). If at any station this stress exceeds the proportional elastic limit of the material at the temperature at this station, then plastic flow takes place, and it becomes necessary to resort to a trial-and-error procedure to adjust the stresses to allow for this flow.

Assume, for example, the equivalent uniaxial stress at a given station lies at point A on the extension of the modulus line in figure 2. Because the point A lies above the proportional elastic limit (point B), plastic flow must occur. The stress and the strain must be adjusted to fall on the curved stress-strain curve that is characteristic of the material. As a starting point, the total strain in the true stress-strain condition is assumed equal to the strain at A. The stress-strain condition at the given station then lies on the constant-strain line through B, or at C. The plastic strain $\epsilon_{p,n}$ is
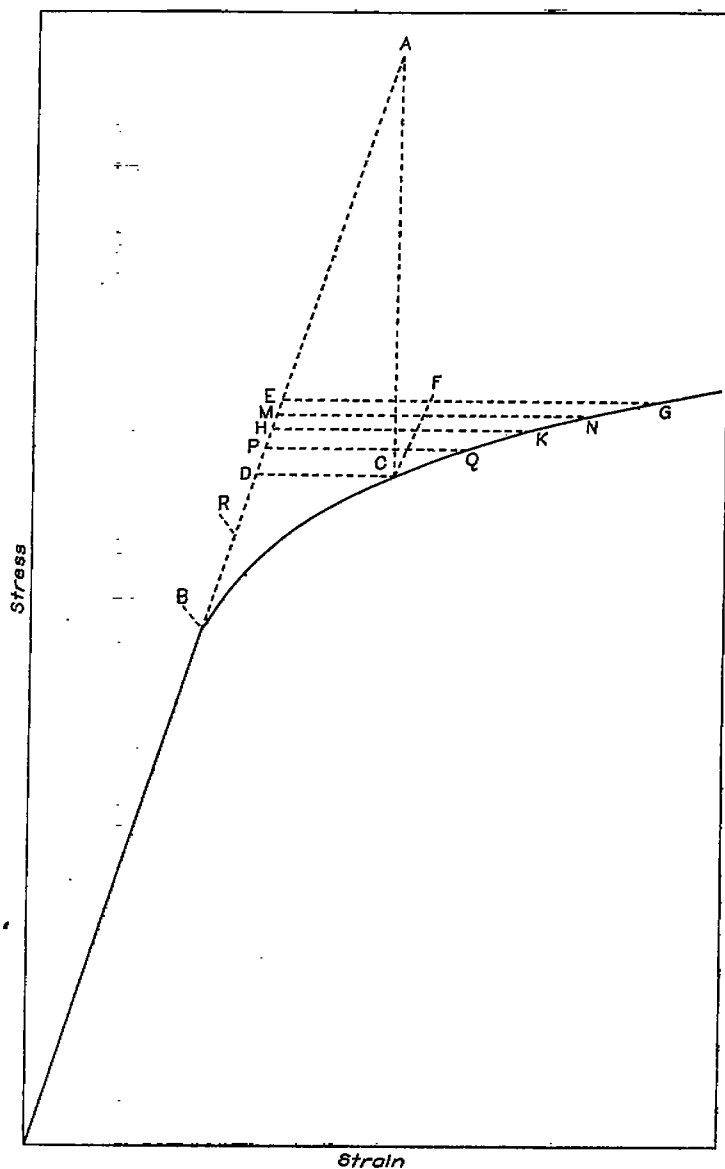

FIGURE 2.—Uniaxial stress-strain curve illustrating procedure used to find correct value of plastic strain.

given by CD. Values of $\Delta_{r,n}$, $\Delta_{t,n}$, and P'_n may be obtained by using this value of $\epsilon_{p,n}$, together with the values of $\sigma_{r,n}$, $\sigma_{t,n}$, and $\sigma_{e,n}$ from the elastic calculations.

Once P'_n has been calculated, new values of $\sigma_{r,n}$, $\sigma_{t,n}$, and $\sigma_{e,n}$ can be computed. The new value of $\sigma_{e,n}$ is greater than that at point D, such as that at point E. Although the stresses corresponding to $\sigma_{e,n}$ at point E together with the strain CD meet the conditions of equations (9) and (10), they locate the stress-strain point F, which is not on the stress-strain curve, so that the physical conditions imposed by the material are as yet unsatisfied. Inasmuch as any value of $\epsilon_{p,n}$ less than CD would give a value of $\sigma_{e,n}$ greater than that at E, CD is a lower limit of $\epsilon_{p,n}$. Similarly, because the value of $\sigma_{e,n}$ calculated by using an $\epsilon_{p,n}$ of CD is too great, the increment of strain EG corresponding to this $\sigma_{e,n}$ is an upper limit of $\epsilon_{p,n}$. Inasmuch as the true value of $\epsilon_{p,n}$ lies between CD and EG, their numerical average, shown as HK, is assumed to be a good approximation. New values of P'_n, $\sigma_{r,n}$, $\sigma_{t,n}$, and $\sigma_{e,n}$ can be computed by using HK for $\epsilon_{p,n}$, the stress at E for $\sigma_{e,n}$, and $\sigma_{r,n}$ and $\sigma_{t,n}$. Assume that this new value of $\sigma_{e,n}$ lies at the point M. Because the stress at M is higher than the stress at H in value, the increment HK is too small a value of $\epsilon_{p,n}$ and is therefore established as a new lower limit of $\epsilon_{p,n}$. Further, because M is less than E, the corresponding increment MN is a new upper limit for $\epsilon_{p,n}$ and the process could be repeated again with the numerical average of MN and HK. Similarly, if the calculation using an $\epsilon_{p,n}$ of HK had resulted in a $\sigma_{e,n}$ at P, HK would constitute a new upper limit and PQ a new lower limit. Had the resulting $\sigma_{e,n}$ been at R, HK would have still become the new upper limit of $\epsilon_{p,n}$, but CD would have remained as the lower limit. The process is repeated until the value of $\epsilon_{p,n}$ used in the computation and the $\epsilon_{p,n}$ corresponding to the resulting $\sigma_{e,n}$ are equal.

Calculation of plastic flow when previous plastic flow has occurred.—The equations for strain that would apply to a disk that had already undergone the plastic strain are

$$\epsilon_r = \frac{\sigma_r - \mu\sigma_t}{E} + \alpha\Delta T + [\Delta_r] + \Delta_r \qquad (21)$$

$$\epsilon_t = \frac{\sigma_t - \mu\sigma_r}{E} + \alpha\Delta T + [\Delta_t] + \Delta_t \qquad (21a)$$

Here the terms $[\Delta_r]$ and $[\Delta_t]$ represent strains already existent in the material before the application of stresses σ_t and σ_r and are constant for the calculation, whereas Δ_r and Δ_t represent the components of plastic strain resulting from the application of σ_r and σ_t. In the solution of the equations by the finite-difference method, a term $[P'_n]$ appears together with term P'_n. When previous plastic flow has occurred only once, $[P'_n]$ is identical with P'_n from the previous calculation; where plastic flow has previously occurred more than once, $[P'_n]$ is the algebraic sum of all earlier P'_n terms. Thus, the previous plastic flow given by $[P'_n]$ may be grouped with the temperature-effect term H'_n by replacing H'_n with $H'_n - [P'_n]$.

This procedure amounts to an assumption that, as the
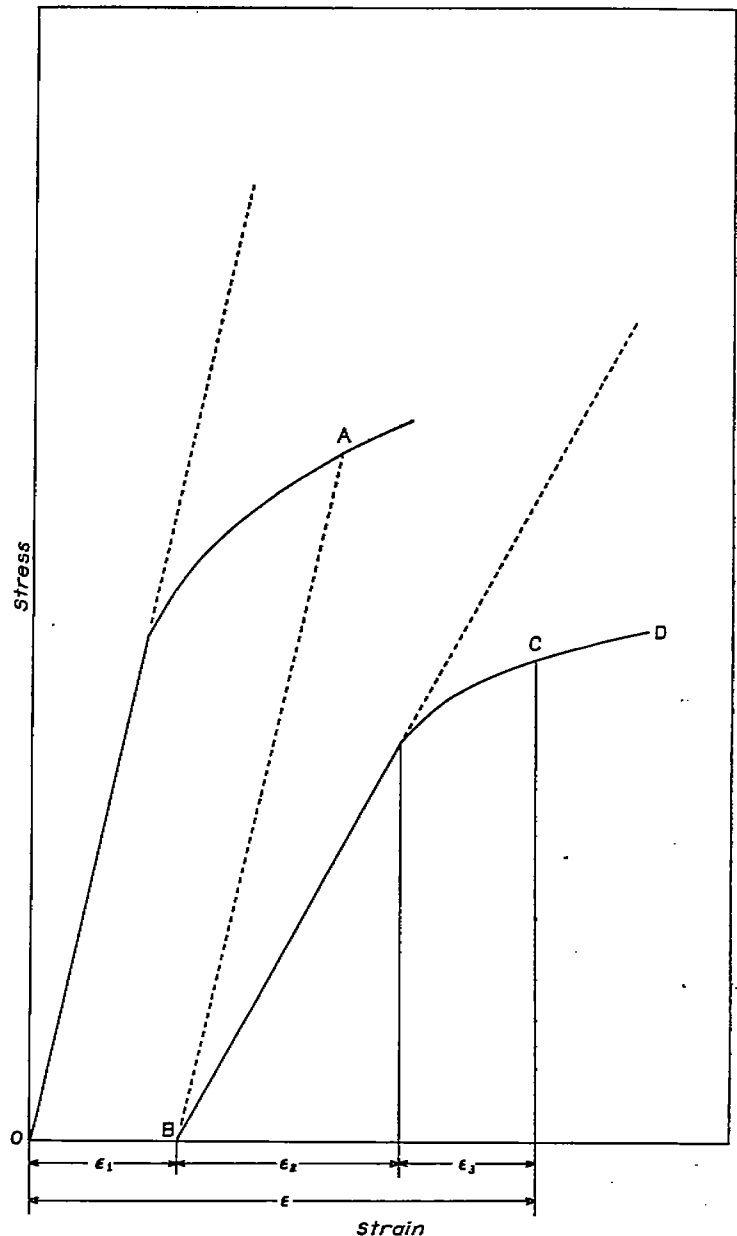
FIGURE 3.—Uniaxial stress-strain curves showing components of strain when plastic flow occurs a second time.

load and the temperature change, the stress position on the new stress-strain curve would be the same as if a test specimen were loaded above the yield point, the load removed, the temperature changed, and a new load applied. This assumption is illustrated by figure 3, in which point A represents a loading at the first temperature condition; the dotted line AB represents the load-removal path; the curve BCD, the stress-strain curve at the new temperature; and point C, the new stress position. The total strain at point C is given by the sum of three strains. The residual strain caused by the first loading is ϵ_1; ϵ_2 is the elastic part of the strain caused by the second loading; and ϵ_3, the plastic strain caused by the second loading.

When the foregoing procedure is applied, the curve BCD must, of course, represent the true stress-strain curve at the new temperature of a material that has already been subjected to the plastic cycle OAB. In general, the new stress-strain curve is different from the stress-strain curve at the

FIGURE 4.—Typical deformation-time curve from a constant-temperature, constant-load creep test.

given temperature of a material that has not been subjected to plastic flow; however, unless data are available it may be necessary to assume that the curve BCD is the stress-strain curve at the given temperature of a specimen of virgin material.

Calculation of effect of creep.—Creep is usually defined as the continuous deformation of material under a continuously applied load. Experimental data on creep of various materials are usually obtained from tests r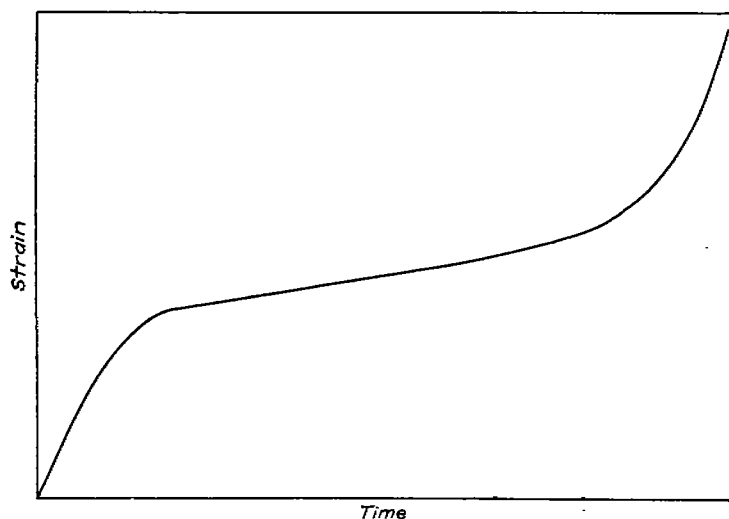un under constant load and temperature, although in many engineering applications of materials the more general problem of changing load and temperature must be considered. The deformation curve obtained in a typical test is shown in figure 4. From this figure it can be seen that the deformation may be considered as having occurred in three stages. During the primary stage, the deformation proceeds at a decreasing rate; during the secondary stage, at a constant rate; and during the tertiary stage, at an increasing rate, which proceeds until failure occurs.

Because of the lack of data on creep except for uniaxial tensile stress, a relation between creep deformation and stress must be assumed. The following equations have been used for calculations in this report but, as better data become
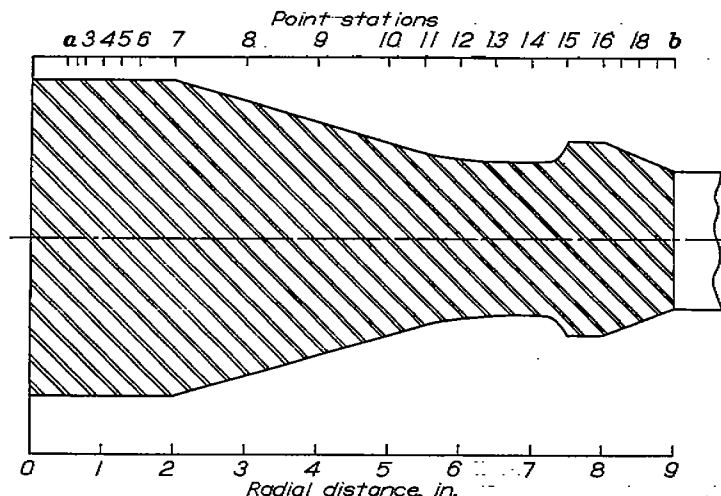

FIGURE 5.—Cross section of disk used for numerical examples showing location of point stations.

available, more accurate relations can be used. By the use of reasoning similar to that employed in determining the biaxial components of plastic-strain formulas for the creep increments, $\delta_{r,n}$ and $\delta_{t,n}$ may be written

$$\delta_{r,n}=\frac{\Gamma_n}{2\sigma_{e,n}}(2\sigma_{r,n}-\sigma_{t,n}) \qquad (22)$$

$$\delta_{t,n}=\frac{\Gamma_n}{2\sigma_{e,n}}(2\sigma_{t,n}-\sigma_{r,n}) \qquad (22a)$$

In equations (22) and (22a), Γ_n represents the total creep that would occur in time τ under the uniaxial stress $\sigma_{e,n}$. It is here assumed that for sufficiently small values of τ the creep may be considered as occurring instantaneously at the end of the time period.

During the secondary stage of creep, a characteristic creep rate c_n exists, corresponding to the stress $\sigma_{e,n}$ at temperature T, and Γ_n is given directly by

$$\Gamma_n=c_n\tau \qquad (23)$$

This rate is the value usually published in papers on creep and is the rate used for the numerical calculations of this report. During primary and tertiary creep stages, the creep rate is also a function of time, but does not otherwise complicate the computation.

Once values of $\delta_{r,n}$ and $\delta_{t,n}$ have been found, the values of the Q'_n terms may be determined and new values of $\sigma_{r,n}$ and $\sigma_{t,n}$ may be computed. If the computed values of $\sigma_{r,n}$ and $\sigma_{t,n}$ differ by more than a small amount, perhaps 2 percent, from the values of these stresses before creep occurred, a shorter time interval should be selected and additional computations made for each such time interval required to equal the total time during which creep occurs. The effect of creep that occurred at previous time intervals is considered in a manner similar to that employed in considering previous plastic flow. The successive values of Q'_n are summed to form a term $[Q'_n]$, which gives the total effect of all previous creep deformation so that the term

$$H'_n-[P'_n]$$

is replaced by

$$H'_n-[P'_n]-[Q'_n]$$

In any calculation of stress distribution subsequent to the occurrence of creep, the creep term $[Q'_n]$ is combined with the term $[P'_n]$ as the cumulative effect of all previous plastic deformation.

Examples showing in detail how successive stages of plastic flow and creep are computed, each stage considering all previous plastic deformation, are given in the following section.

NUMERICAL EXAMPLES

The numerical examples presented here represent a set of computations during one complete start-run-stop cycle for a typical turbine disk with a continuous rim and welded blades. The assumed profile of the disk is shown in figure 5, together with the locations of the point stations used in the computations. The assumed temperature distributions and corre-

sponding turbine rotative speeds are shown in figure 6. Curve IV and ·the corresponding speed of 11,500 rpm represent the steady-state running condition. Curves I to III and the corresponding speeds represent running conditions through which the turbine disk passes in reaching steady-state operation. Curves V to VII together with the respective speeds represent running conditions through which the turbine disk passes when being stopped. Creep is assumed to occur only during the steady-state running period.

The physical properties of the disk material, including specific gravity, modulus of elasticity, stress-strain characteristics, and thermal coefficients of expansion, were based on the data appearing in reference 6, together with unpublished data obtained from the author of this reference. The stress-strain curves were constructed on the basis of these data and those for example I appear in figure 7. Inasmuch as no data were available on the effect of previous plastic flow on the shape of the stress-strain curves, it was necessary to ignore such effects and to use curves obtained directly from simple tensile-test data. Creep properties corresponding to a material having good creep resistance were assumed. The effect of primary creep was omitted because of lack of data.

Because the disk used for these calculations is solid at the center, a supplementary numerical example showing the computation of the plastic-flow effect on stress distribution in a disk containing a central hole is given in the appendix.

Example I.—Example I is the calculation of the stress distribution in a disk operating under the conditions of curve I of figure 6 and having been subjected to no previous plastic deformation. These conditions are assumed to represent disk operation after the first short period of steady combustion when gas temperatures are high, thereby establishing a steep temperature gradient between the center and the rim of the disk.

The preliminary elastic calculation is carried out in table I (a) by the method of reference 1. Two changes are made in the tabular setup. The first change is the insertion of columns 25a and 25b immediately following column 25. Column 25a lists the accumulated values of $[P'_n]$ and $[Q'_n]$, the total effect of previous plastic deformation. For the present example, this column is zero for all stations. Column 25b is the value of the term $H'_n-[P'_n]-[Q'_n]$, which in
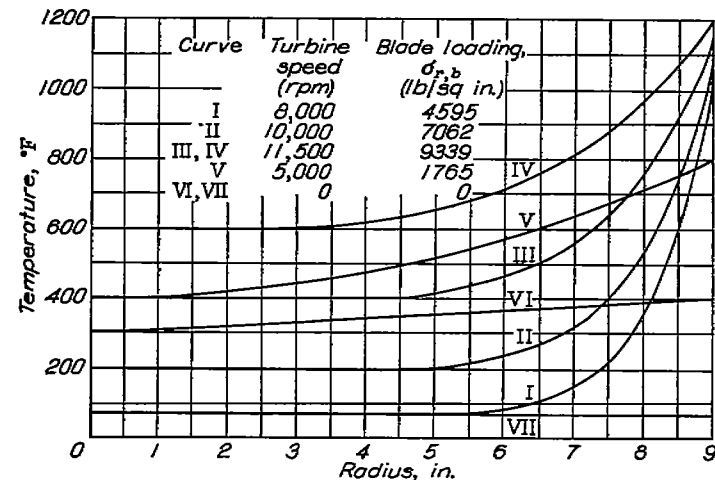
this example is the same as column 25. The second change is the computation of M_n and M'_n (columns 31 and 32, respectively), which were computed in reference 1 by the use of column 25. In the present computations, column 25b is used. In addition, two more columns, 40 and 41, are added. Column 40 lists the values of the proportional elastic limit $\sigma_{y,n}$ of the material and column 41 lists the values of $\sigma_{e,n}$ as computed from equation (18). The entries in columns 40 and 41 of table I (a) show that the equivalent stress $\sigma_{e,n}$ is less than $\sigma_{y,n}$ for all point stations except 17 to b. The effect of plastic flow must be considered at these stations and flow at these stations modifies the stresses at other locations in the disk. With the exceptions and the additions noted, the method of computation is the same as the method of reference 1 and will not be discussed in further detail.

The plastic-flow calculation has been divided into two parts because several quantities used in the computation depend only on the dimensions of the disk and can be used in all subsequent calculations involving plastic deformation. These quantities are computed for stations 17 to b, as shown by the four column headings of table I (b).

The second part of the plastic-flow calculation is given in table I (c). The first column in this part of the table (column 46) lists the values of $\epsilon_{p,n}$ obtained from the corresponding stress-strain curve (fig. 7), as previously explained. Column 46a lists the value of $\epsilon_{p,n}$ used for the ensuing calculation, which for the first approximation is the same as column 46.
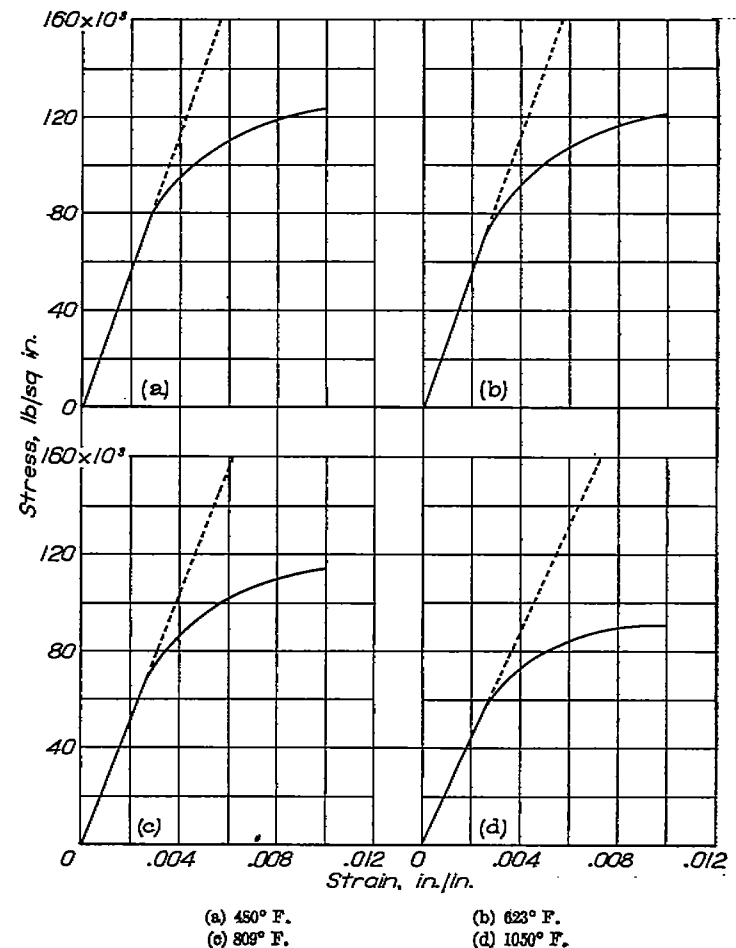
FIGURE 7.—Stress-strain curves of disk material for various temperatures.

(a) 450° F.   (b) 623° F.
(c) 809° F.   (d) 1050° F.

FIGURE 6.—Assumed temperature-distribution curves and corresponding turbine speeds. (Curves I, II, and III are consecutive starting conditions; curve IV represents steady-state operation; and curves V, VI, and VII are consecutive stopping conditions.)

Curve	Turbine speed (rpm)	Blade loading, $\sigma_{r,b}$ (lb/sq in.)
I	8,000	4595
II	10,000	7062
III, IV	11,500	9339
V	5,000	1765
VI, VII	0	0

Columns 47 and 48 list the values of $\Delta_{r,n}$ and $\Delta_{t,n}$, respectively, computed by equations (20). Columns 49 to 52 are computed as shown by the column headings and from these columns the values of P'_n are computed and listed in column 53. Column 54 gives the values of the term $H'_n-[P'_n]-[Q'_n]-P'_n$, which is then used to compute new values of M_n, M'_n, $B_{r,n}$, $B_{t,n}$, $\sigma_{t,a}$, $\sigma_{r,n}$, $\sigma_{t,n}$, and $\sigma_{e,n}$ as shown in columns 55 to 62, respectively. The new values of $\epsilon_{p,n}$ corresponding to the new values of $\sigma_{e,n}$ are read from figure 7 and listed in column 46 of the second-approximation calculation. The values in column 46 for the first and second approximations now constitute the lower and upper limits, respectively, of the possible strain increments. For the second approximation, column 46a therefore lists as the values of $\epsilon_{p,n}$ to be used in this set of calculations the numerical averages of the two sets of readings from the stress-strain curve. From this value, another new set of stress values is computed and a third set of readings listed in column 46.

At this point in the calculation, two alternate procedures are possible, as shown by consideration of station b. Inasmuch as the average value of 4300×10^{-6} inches per inch used in the second approximation gave a graph reading of 1900×10^{-6} inches per inch, the averaging procedure would indicate that the next trial should be $\dfrac{4300+3960}{2}\times10^{-6}$ or 4130×10^{-6} inches per inch. This value could be used and the procedure continued until the correct value is found. Considerable time may be saved, however, in making the calculation if a weighted approximation is used. Because the plastic-strain value of 3960×10^{-6} inches per inch gave a resulting reading of 4650×10^{-6} inches per inch whereas the value 4300×10^{-6} inches per inch gave the reading 1900×10^{-6} inches per inch, the strain 3960×10^{-6} inches per inch is apparently more nearly correct than 4300×10^{-6} inches per inch. In addition, the shape of the stress-strain curve in the region of 3960×10^{-6} is such that small increases in stress correspond to large changes in strain. If a trial calculation were
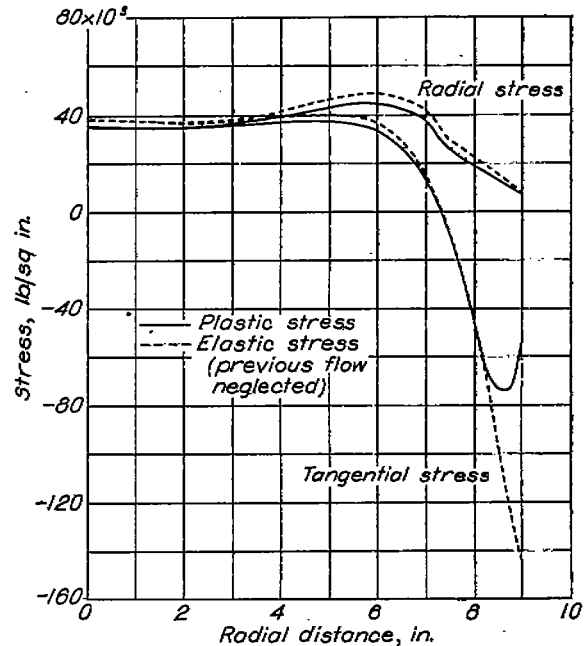
FIGURE 9.—Stresses in turbine disk under conditions of curve II of figure 6.

made using a value closer to 3960 than 4130 (for instance, 4000), more information might be obtained than would be obtained by the averaging procedure. The right answer is thereby more quickly obtained. The same reasoning might be applied to the selection of values to be used at the other stations for the third calculation. The second of these two procedures has been used in table I (c), as can be seen from the values of $\epsilon_{p,n}$ in column 46a used for the third approximation.

Completion of the third approximation and comparison with new values of strain obtained from the stress-strain curve show the estimates of the third approximation to be nearly correct, so that small adjustments made to compute the fourth and fifth approximations give the final answers. A calculation equivalent to a sixth approximation is then made to column 53 to get the final correct values of the P'_n terms. The stresses at the other stations a through 16 can now be computed by using the value of $\sigma_{t,a}$ found in the sixth approximation with the values $A_{r,n}$, $A_{t,n}$, $B_{r,n}$, and $B_{t,n}$ found in table I (a). The values of plastic stress at all radii together with the elastic-stress distribution are plotted in figure 8.

Example II.—Example II considers the disk studied in example I at the time that the operating conditions have reached those indicated by curve II of figure 6. The elastic calculations are made by the method of reference 1 modified in accordance with the changes made in example I. The essential parts of the computation are shown in table II, which is abridged from the complete calculation. Column 25a lists the values of $[P'_n]$ that were found as the final values of P'_n in example I. Plastic flow occurs at stations 17, 18, 19, and b, and calculated true stresses when this plastic flow is considered are listed in table II. The stresses obtained as a result of this computation are plotted in figure 9. The elastic stresses obtained without considering the plastic flow that occurred previously are also plotted for comparison in figure 9.

Example III.—Example III continues the cycle analyzed in examples I and II, at the conditions of curve III of figure 6.
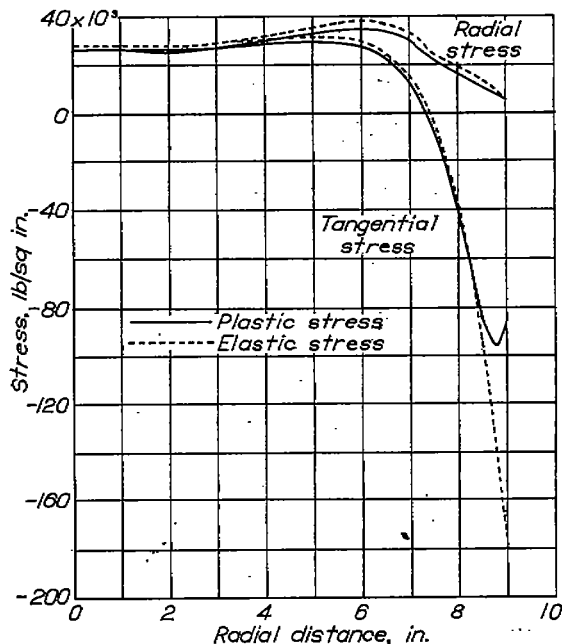

FIGURE 8.—Stresses in turbine disk under conditions of curve I of figure 6.
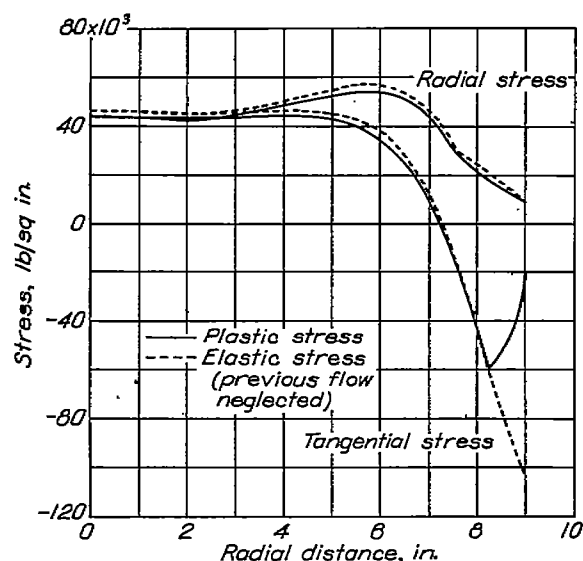
FIGURE 10.—Stresses in turbine disk under conditions of curve III of figure 6.

Table III gives the essential parts of the calculation for this example, which is similar to the procedure for example I in table I. The value of $[P'_n]$, column 25a, however, is the total of the values of P'_n obtained from examples I and II. In this example, plastic flow occurs only at stations 17 and 18. The results of this computation, together with the elastic-stress curves found without consideration of previous plastic flow, are shown in figure 10.

Example IV.—The steady-state operating conditions represented by curve IV of figure 6 are treated in example IV. The essential calculations shown in table IV (a) were made similarly to those in table III except that $[P'_n]$ in column 25a is now the sum of the values of P'_n from examples I, II, and III. Because no values of $\sigma_{e,n}$ exceed those of $\sigma_{y,n}$, no plastic flow occurs and the stress values of table IV (a) are the true stresses at the beginning of steady-state operation. However, as parts of the disk are at elevated temperature, significant creep can occur at steady load at stations 16, 17, and 18 where the stresses are sufficiently high. Table IV (b) shows the calculations of creep. Column 63 lists the creep rate c_n (in./(in.)(hr)), and column 64 the creep increment Γ_n for the 5-hour running period. Columns 65 and 66 give the computed values of $\delta_{r,n}$ and $\delta_{t,n}$, respectively. The computation
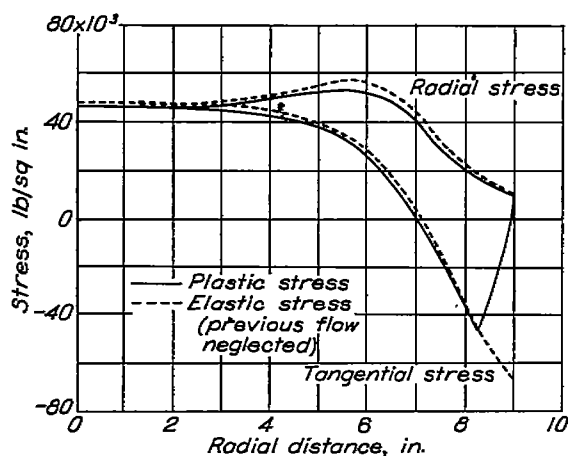
FIGURE 11.—Stresses in turbine disk under conditions of curve IV of figure 6. (The stresses before and after creep occurs coincide within the accuracy of this plot.)
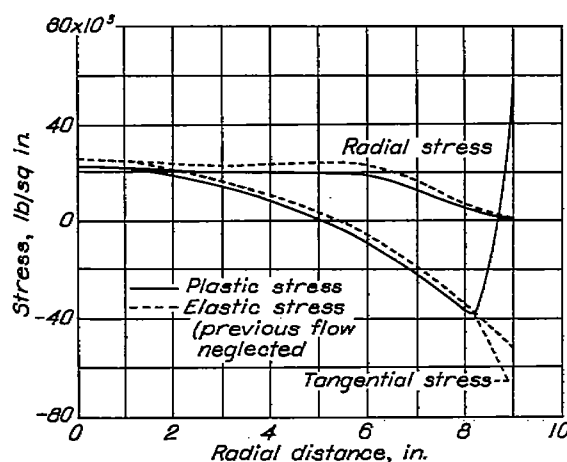
FIGURE 12.—Stresses in turbine disk under conditions of curve V of figure 6.

then proceeds in a manner similar to the plastic-flow calculations, as indicated in the column headings. The values for stress obtained indicate that, for small values, creep has only a slight effect on the stresses. Figure 11 shows the stress distributions at the beginning and the end of the steady-state running period, together with the elastic stresses obtained without considering either creep or previous plastic flow.

Example V.—The conditions of example V represent one of the conditions through which the turbine disk is assumed to pass during the stopping period. The abridged elastic calculations are given in table V. Values listed now represent the accumulated effect of plastic flow $[P'_n]$ plus the additional effect of the creep represented by $[Q'_n]$; $[Q'_n]$ is the same as the Q'_n computed in example IV. All values of $\sigma_{e,n}$ are less than the corresponding values of $\sigma_{y,n}$; therefore no plastic flow occurs. The results of the calculation are plotted in figure 12, together with the elastic stresses computed without considering previous plastic flow or creep.

Example VI.—Example VI is the computation of the stress distribution at the temperature distribution assumed to be present shortly after the wheel has stopped turning. The essential parts of the calculation are shown in table VI. Because no flow was found in example V, the $[P'_n]+[Q'_n]$ term will be the same in this example as in example V. Plastic flow occurs at station b. The resulting stresses are plotted in figure 13, together with the elastic stresses com-
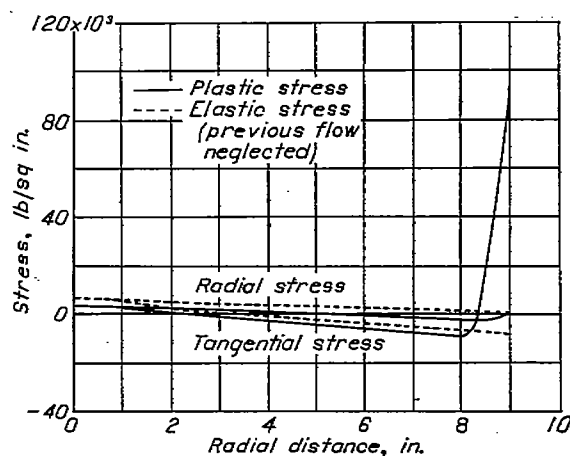
FIGURE 13.—Stresses in turbine disk under conditions of curve VI of figure 6.

puted without consideration of previous plastic flow and creep.

Example VII.—Example VII is the computation of the stress distribution in the disk after the temperature has become uniform at the ambient temperature (assumed to be 70° F) throughout the disk. These stresses are therefore the residual stresses in the disk resulting from the flow occurring during the complete operating cycle. The abridged calculations given in table VII indicate that plastic flow occurs at station b and the residual stresses are plotted in figure 14.

Discussion of numerical examples.—The foregoing cycle of stress calculations is indicative of the means of obtaining a complete analysis of the stress behavior of a turbine disk. Although the results plotted in the various figures and summarized in figure 15 do not represent the exact behavior of any particular turbine disk because of the lack of data on the material properties and temperature gradients, they do give a qualitative picture of the behavior of a turbine disk with welded blades. The high residual tensile stress at the rim of the wheel provides a plausible explanation of the rim cracking that has occurred in such wheels. The compressive flow at the rim during starting and the tensile flow on stopping result in cyclic flow of the rim material with each start and stop and possibly induce cracks. When accurate data are available on creep, stress-strain relations, the effect of strain-hardening, and temperature distribution, quantitative

FIGURE 15.—Plastic tangential stresses in turbine disk during one running cycle.

analyses of disk behavior will be available as a guide in future turbine design.

CONCLUSIONS

A method for studying the operating stresses in gas-turbine disks has been presented that includes consideration of the effect of plastic flow and creep on the stress distribution. Results of calculations indicate that rim cracking in turbine wheels with welded blade attachments may be caused by alternate compressive and tensile plastic flow as the wheel is alternately heated and cooled. From the results of the numerical examples presented, it may be concluded that plastic flow markedly alters the elastic-stress distribution.

Flight Propulsion Research Laboratory,
    National Advisory Committee for Aeronautics,
        Cleveland, Ohio, *March 5, 1948.*

FIGURE 14.—Residual stresses in turbine disk upon completion of one operating cycle.

APPENDIX

STRESS CALCULATION FOR DISK WITH CENTRAL HOLE

The calculations given in the section Numerical Examples deal with a disk that is solid at the center and has temperature gradients such that the plastic flow is confined to the region of the rim. Disks of other types spun under different conditions may be subject to plastic flow in other regions.

One example of such a disk is a parallel-sided disk with a
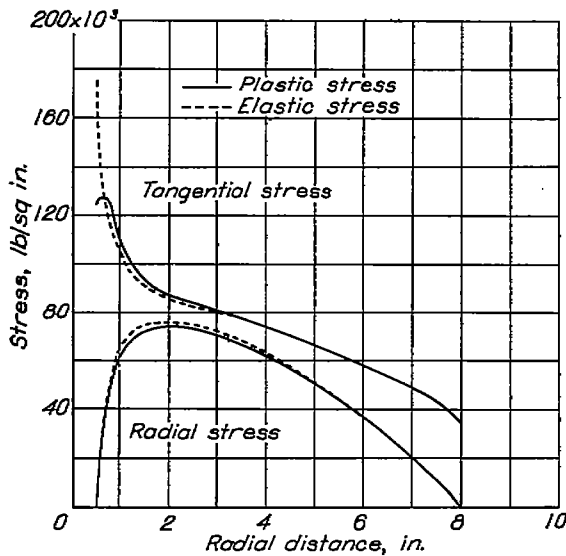
FIGURE 16.—Stresses in parallel-sided disk with central hole.

central hole spun at a uniform temperature. In this disk plastic flow first occurs in the region of the central hole. Such a disk spun at a speed great enough to cause some flow near the hole is calculated here.

The essential columns of the elastic calculation are given in table VIII (a). Flow is indicated at stations a, 2, 3, and 4. However, as flow occurs the stresses farther out in the disk may be increased. The quantities depending on disk dimensions, together with the first approximation, shown in table

VIII (b), are found in the manner given in the text. When the values of $B_{r,n}$ and $B_{t,n}$ (columns 57 and 58) are found for the stations at which flow occurs, however, new values of $B_{r,n}$ and $B_{t,n}$ must also be computed for all other point stations before a new value of $\sigma_{t,a}$ (column 59) can be found. These computations are also shown in table VIII (b) for the first approximation. Additional approximations must be made in the same manner until the correct flow increments are found. The stresses so calculated are plotted in figure 16.

Where large numbers of computations involving plastic flow at the center of the disk are to be made, it may be desirable to change the finite-difference approach to the problem in such a manner that the calculations are made from the outside of the disk toward the center instead of from the center toward the rim. This procedure has certain disadvantages as a general approach to the problem of stresses in disks, particularly in that it requires a greater number of significant figures to obtain the same accuracy. For special applications it may, however, present advantages that outweigh the disadvantages in more general problems.

REFERENCES

1. Manson, S. S.: The Determination of Elastic Stresses in Gas-Turbine Disks. NACA Rep. 871, 1947.
2. Thompson, A. Stanley: Stresses in Rotating Disks at High Temperatures. Jour. Appl. Mech., vol. 13, no. 1, March 1946, pp. A45–A52.
3. Nadai, A.: Plasticity. McGraw-Hill Book Co., Inc., 1931, pp. 72–74.
4. Soderberg, C. Richard: The Interpretation of Creep Tests for Machine Design. A.S.M.E. Trans., vol. 58, no. 8, Nov. 1936, pp. 733–743.
5. Taylor, G. I., and Quinney, H.: The Plastic Distortion of Metals. Phil. Trans. Roy. Soc. London, ser. A., vol. 230, Feb. 1932, pp. 323–362.
6. Fleischmann, Martin: 16–25–6 Alloy for Gas Turbines. Iron Age, vol. 157, no. 3, Jan. 17, 1946, pp. 44–53; cont., vol. 157, no. 4, Jan. 24, 1946, pp. 50–60.

TABLE I.—CALCULATION OF STRESS DISTRIBUTION FOR EXAMPLE I

(a) Elastic-stress calculation

n	1	2	3	4	5	6	7	8	9	10	11	12	13	14	15
	r_n	h_n	$\rho_n \omega^2$	μ_n	E_n	α_n	ΔT_n	C_n $(1)\times(2)$	$\frac{(1)-(1)_{n-1}}{2}$	D_n $(2)\times(9)$	G_n $(2)_{n-1}\times(9)$	$(3)\times(8)\times (1)$	$(12)+ (12)_{n-1}$	H_n $(9)\times(13)$	$1/(5)$
a__	0.5000	4.3750			30.400×10⁶	8.2970×10⁻⁶	0	2.1875				584.86			0.032895×10⁻⁶
2__	.6250	4.3750			30.400	8.2970	0	2.7844	.06250	0.27344	0.27344	913.85	1,498.7	93.672	.032895
3__	.7500	4.3750			30.400	8.2970	0	3.2812	.06250	.27344	.27344	1,315.9	2,229.8	139.36	.032895
4__	1.0000	4.3750			30.400	8.2970	0	4.3750	.12500	.54688	.54688	2,339.4	3,655.3	456.92	.032895
5__	1.2500	4.3750			30.400	8.2970	0	5.4688	.12500	.54688	.54688	3,655.4	5,994.8	749.37	.032895
6__	1.5000	4.3750			30.400	8.2970	0	6.5625	.12500	.54688	.54688	5,263.8	8,919.2	1,114.9	.032895
7__	2.0000	4.3750	Constant at 524.78	Constant at 0.85000	30.400	8.2970	0	8.7500	.25000	1.0938	1.0938	9,357.8	14,622	3,656.4	.032895
8__	3.0000	3.8400			30.400	8.2970	0	11.520	.50000	1.9200	2.1875	18,480	27,838	18,919	.032895
9__	4.0000	3.2750			30.400	8.2970	0	13.100	.50000	1.6375	1.9200	28,020	46,500	23,250	.032895
10_	5.0000	2.6800			30.300	8.3020	3.00	13.400	.50000	1.3400	1.6375	35,827	63,847	31,923	.033003
11_	5.5000	2.3720			30.300	8.3080	7.00	13.048	.25000	.59300	.67000	38,368	74,195	18,548	.033003
12_	6.0000	2.2100			30.200	8.3240	17.00	13.260	.25000	.55250	.59300	42,543	80,911	20,228	.033112
13_	6.5000	2.1600			30.100	8.3580	38.00	14.040	.25000	.54000	.55250	48,799	91,342	22,836	.033222
14_	7.0000	2.1550			30.000	8.4240	79.00	15.085	.25000	.53875	.54000	56,467	105,270	26,317	.033333
15_	7.5000	2.7000			29.600	8.5500	158.00	20.250	.25000	.67500	.53875	81,212	137,680	34,420	.033784
16_	8.0000	2.7000			28.900	8.7810	302.00	21.600	.25000	.67500	.67500	92,401	173,620	43,404	.034602
17_	8.2500	2.5500			28.400	8.9550	410.00	21.038	.12500	.31875	.33750	92,808	185,210	23,151	.035211
18_	8.5000	2.3800			27.500	9.1840	553.00	20.230	.12500	.29750	.31875	91,952	184,760	23,095	.036364
19_	8.7500	2.1450			26.000	9.4820	739.00	18.769	.12500	.26312	.29750	87,819	179,770	22,471	.039162
b__	9.0000	1.9100			22.100	9.8690	980.00	17.190	.12500	.23875	.26312	82,728	170,550	21,319	.045249

n	16	17	18	19	20	21	22	23	24	25	25a
	$(4)\times(15)$	$\frac{[1+(4)]\times(15)}{(1)}$	$(17)\times(9)$	$(17)_{n-1}\times(9)$	C'_n $(16)+(18)$	D'_n $(16)+(18)$	F'_n $(16)_{n-1}-(19)$	G'_n $(16)_{n-1}-(19)$	$(6)\times(7)$	H'_n $(24)-(24)_{n-1}$	$[P'_n]+ [Q'_n]$
a__	0.011513×10⁻⁶	0.088816×10⁻⁶							0 ×10⁻⁶	×10⁻⁶	
2__	.011513	.071053	0.0044410×10⁻⁶	0.0055510×10⁻⁶	0.015954×10⁻⁶	0.037336×10⁻⁶	0.0069620×10⁻⁶	0.027344×10⁻⁶	0	0	
3__	.011513	.059211	.0037010	.0074010	.015214	.036596	.0070720	.028454	0	0	
4__	.011513	.044408	.0055510	.017064	.017064	.038446	.0041120	.025494	0	0	
5__	.011513	.035526	.0044410	.0055510	.015954	.037336	.0059620	.027344	0	0	
6__	.011513	.029605	.0037010	.0044410	.015214	.036596	.0070720	.028454	0	0	
7__	.011513	.022204	.0055510	.0074010	.017064	.038446	.0041120	.025494	0	0	
8__	.011513	.014803	.0074010	.011102	.018914	.040296	.00041100	.021793	0	0	
9__	.011513	.011102	.0055510	.0074010	.017064	.038446	.0041120	.025494	0	0	
10_	.011551	.0089108	.0044510	.0055510	.016006	.037458	.0059620	.027844	24.906	24.906	
11_	.011551	.0081007	.020250	.0022280	.013576	.035028	.0093230	.030775	58.156	33.250	
12_	.011589	.0074502	.0018630	.020250	.013452	.034975	.0095260	.030978	141.508	83.352	
13_	.011628	.0069000	.0017250	.0018630	.013358	.034947	.0097260	.031249	317.604	176.10	
14_	.011667	.0064286	.0016070	.0017250	.013274	.034940	.0099030	.031497	665.496	347.89	
15_	.011824	.0060611	.0015200	.0016070	.013344	.035304	.010060	.031726	1350.90	685.40	
16_	.012111	.0058391	.0014600	.0015200	.013571	.036062	.010304	.032264	2651.86	1301.0	
17_	.012324	.0057618	.0007200	.00073000	.013044	.035931	.011381	.033872	3671.55	1019.7	
18_	.012727	.0057754	.00072200	.00072000	.013449	.037086	.011604	.034491	5078.75	1407.2	
19_	.013462	.0059342	.00074200	.00072200	.014204	.039204	.012005	.035642	7007.20	1928.4	
b__	.015837	.0067873	.00084800	.00074200	.016685	.046097	.012720	.037720	9671.62	2664.4	Constant at 0

n	25b	26	27	28	29	30	31	32	33	34	35
	$H_n-[P'_n]-[Q'_n]$, $(25)-(25a)$	$(20)\times(10)- (8)\times(21)$	K_n, $[(22)\times(10)- (8)_{n-1}\times(21)]+ (26)$	L_n, $[(23)\times(10)+ (11)\times(21)]+ -(26)$	K'_n, $[(8)\times(22)- (20)\times(8)_{n-1}]+ -(26)$	L'_n, $[(20)\times(11)+ (8)\times(23)]+ -(26)$	M_n, $[(25b)\times(10)+ (14)\times(21)]+ (26)$	M'_n, $[(20)\times(14)+ (8)\times(25b)]+ (26)$	$A_{r,n}$, $(27)\times(33)_{n-1}+ (28)\times(34)_{n-1}$	$A_{t,n}$, $(29)\times(33)_{n-1}+ (30)\times(34)_{n-1}$	$B_{r,n}$, $(27)\times(35)_{n-1}+ (28)\times(36)_{n-1}+ (31)$
a__	×10⁻⁶	×10⁻⁶							1.0000	1.0000	0
2__	0	−0.097729×10⁻⁶	0.81902	0.18097	0.19029	0.80971	−35.786	−15.292	.99999	1.0000	−35.786
3__	0	−.11592	.84657	.15344	.15870	.84130	−43.996	−18.290	1.0000	1.0000	−76.638
4__	0	−.15887	.77988	.22010	.23919	.76080	−110.57	−49.077	.99998	.99999	−178.45
5__	0	−.19546	.81001	.18097	.19029	.80970	−143.14	−61.166	.99996	.99993	−306.50
6__	0	−.23184	.84657	.15344	.15870	.84131	−175.99	−73.163	.99997	.99999	−401.97
7__	0	−.31774	.77990	.22011	.23920	.76080	−442.30	−196.81	.99998	.99999	−861.33
8__	0	−.42790	.82216	.30379	.37570	.68341	−1310.8	−615.25	1.1259	1.0591	−2,173.8
9__	0	−.47570	.91689	.24298	.30000	.77094	−1879.1	−834.01	1.2896	1.1543	−4,185.0
10_	24.906	−.48049	1.0046	.20391	.27012	.81712	−1558.1	−1,758.6	1.5309	1.2915	−7,267.8
11_	33.250	−.44892	1.0333	.092930	.13430	.91461	−1491.2	−1,527.2	1.7019	1.3868	−9,457.7
12_	83.352	−.45634	.98824	.082955	.10777	.91762	−1651.2	−3,018.3	1.7971	1.4580	−11,579
13_	176.10	−.48345	.94766	.074844	.083789	.92277	−1847.4	−5,744.9	1.8120	1.4941	−13,603
14_	347.89	−.51992	.93326	.068927	.071127	.92764	−2129.1	−10,766	1.7041	1.5149	−15,952
15_	685.40	−.70590	.74482	.057282	−.0034293	.92030	−2376.8	−20,313	1.4231	1.3850	−16,800
16_	1301.0	−.76978	.93962	.059913	.067872	.91728	−3174.2	−37,271	1.4208	1.3697	−20,718
17_	1019.7	−.75176	1.0276	.030493	.058290	.95376	−1558.9	−28,938	1.5013	1.3903	−25,257
18_	1407.2	−.74625	1.0409	.029591	.064578	.94076	−1708.7	−38,504	1.6037	1.4011	−31,137
19_	1928.4	−.73201	1.0791	.028988	.084733	.91985	−1909.8	−49,881	1.7712	1.4244	−39,567
b__	2664.4	−.78842	1.0935	.027099	.11980	.82809	−2053.3	−58,543	1.9754	1.3918	−50,232

TABLE I.—CALCULATION OF STRESS DISTRIBUTION FOR EXAMPLE I—Concluded

(a) Elastic-stress calculation—Concluded

n	36 $B_{t,n}$ $(29)\times(35)_{n-1}+$ $(30)\times(36)_{n-1}+$ (32)	37 $[\sigma_{t,t}-(35)_b]$ $+(33)_b$	38 $(33)\times(37)+$ (35)	39 $(34)\times(37)$ $+(36)$	40 $\sigma_{y,n}$	41 $\sqrt{(38)^2+(39)^2}$ $-(38)\times(39)$
a...	0		27,755	27,755	73,500	27,755
2...	−15.292		27,719	27,740	73,500	27,730
3...	−36.834		27,678	27,718	73,500	27,608
4...	−95.431		27,576	27,659	73,500	27,618
5...	−172.39		27,447	27,582	73,500	27,515
6...	−266.85		27,292	27,488	73,500	27,391
8...	−509.83		26,893	27,245	73,500	27,071
8...	−1,287.3		29,076	28,108	73,500	28,604
9...	−2,478.6	Constant at	31,608	29,559	73,500	30,635
10.	−4,913.8	27,755 for	35,222	30,932	73,500	33,285
11.	−6,997.5	$\sigma_{r,t}$ of 4595	37,779	31,493	73,500	35,061
12.	−10,459	lb/sq in.	38,300	29,952	73,500	34,883
13.	−16,366	(fig. 6)	36,689	25,103	73,500	32,495
14.	−26,915		38,843	15,131	73,500	29,364
15.	−45,028		23,698	−6,504	73,500	27,532
16.	−79,644		18,702	−41,628	73,500	53,490
17.	−106,070		16,412	−67,593	72,000	77,120
18.	−139,980		13,374	−101,090	70,300	108,400
19.	−181,250		9,593	−141,720	67,000	146,750
b...	−213,380		4,595	−174,750	54,000	177,090

(b) Constants determined by disk geometry to be used in all plastic calculations

n	42 $(9)/(1)$	43 $(9)/(1)_{n-1}$	44 $1+(42)$	45 $1-(43)$
17.	0.015152	0.015625	1.0152	0.98438
18.	.014706	.015152	1.0147	.98485
19.	.014286	.014706	1.0143	.98529
b..	.013889	.014286	1.0139	.98571

(c) Plastic-stress calculation

Approximation	n	46 $\epsilon_{p,n}$ (graph reading, fig. 7)	46a $\epsilon_{p,n}$ (estimate)	47 $\frac{\Delta_{r,n}}{(46a)}\times$ $\frac{(62)\times2}{[2(60)-(61)]}$	48 $\frac{\Delta_{t,n}}{(46a)}\times$ $\frac{(62)\times2}{[2(61)-(60)]}$	49 $(47)\times(42)$	50 $(47)_{n-1}\times(43)$	51 $(48)\times(44)$	52 $(48)_{n-1}\times(45)$	53 P'_n $(49)+(50)-$ $(51)+(52)$
1	17	20×10⁻⁶	20×10⁻⁶	13.021×10⁻⁶	−19.657×10⁻⁶	0.19729×10⁻⁶	0.00000×10⁻⁶	−19.956×10⁻⁶	0.000×10⁻⁶	20.153×10⁻⁶
	18	670	670	395.07	−666.15	5.8099	.19729	−675.94	−19.359	662.59
	19	1850	1850	1014.2	−1847.1	14.489	5.8099	−1873.5	−656.35	1237.4
	b	3960	3960	2056.6	−3959.1	28.564	14.489	−4014.1	−1820.7	2236.5
2	17	20	20	12.562	−19.759	.19034	0	−20.059	0	20.249
	18	690	685	402.14	−681.31	5.9139	.19034	−691.33	−19.460	677.97
	19	1880	1865	1040.3	−1860.7	14.862	5.9139	−1887.3	−671.29	1236.8
	b	4650	4300	2312.1	−4295.8	32.113	14.862	−4355.5	−1834.1	2508.4
3	17	20	20	12.544	−19.762	.19007	0	−20.062	0	20.252
	18	670	670	393.05	−666.43	5.7802	.19007	−676.23	−19.463	662.74
	19	1850	1860	1036.5	−1855.8	14.807	5.7802	−1882.3	−656.63	1246.3
	b	1900	4100	2218.3	−4095.2	30.810	14.807	−4152.1	−1829.3	2368.4
4	17	20	20	12.555	−19.760	.19023	0	−20.060	0	20.250
	18	690	680	398.99	−676.36	5.8675	.19023	−686.30	−19.461	672.90
	19	1960	1880	1037.2	−1855.7	14.817	5.8675	−1882.2	−666.42	1236.5
	b	2900	4000	2156.0	−3995.8	29.945	14.817	−4051.3	−1829.2	2266.9
5	17	20	20	12.558	−19.759	.19028	0	−20.059	0	20.249
	18	680	680	399.27	−676.33	5.8717	.19028	−686.27	−19.460	672.87
	19	1860	1860	1037.5	−1855.7	14.822	5.8717	−1882.2	−666.38	1236.5
	b	4200	4015	2160.3	−4011.0	30.004	14.822	−4066.8	−1829.2	2282.4
6	17	20	20	12.557	−19.760	.19026	0	−20.060	0	20.250
	18	680	680	399.25	−676.33	5.8714	.19026	−688.27	−19.461	672.87
	19	1860	1860	1037.5	−1855.7	14.822	5.8714	−1882.2	−666.38	1236.5
	b	4015	4015	2160.8	−4011.0	30.011	14.822	−4066.8	−1829.2	2282.4

Approximation	n	54 $H'_n-[P'_n]-$ $[Q'_n]-P'_n$ $(25b)-(53)$	55 M_n $(54)\times(10)+$ $(14)\times(21)+$ (26)	56 M'_n $(54)\times(8)+$ $(14)\times(20)+$ (26)	57 $B_{r,n}$ $(27)\times(57)_{n-1}+$ $(28)\times(58)_{n-1}+$ (55)	58 $B_{t,n}$ $(29)\times(57)_{n-1}+$ $(30)\times(58)_{n-1}+$ (56)	59 $[\sigma_{t,t}-(57)_b]$ $+(33)_b$	60 $\sigma_{r,n}$ $(33)\times(59)+$ (57)	61 $\sigma_{t,n}$ $(34)\times(59)+$ (58)	62 $\sigma_{s,n}$ $\sqrt{(60)^2+(61)^2}$ $-(60)\times(61)$
Values from elastic-stress calculation, table I (a).	16	1301.0×10⁻⁶	−3174.2	−37,271	−20,718	−79,644	27,755	18,702	−41,628	53,490
	17	1019.7	−1538.9	−28,933	−25,257	−106,070		16,412	−67,593	77,120
	18	1407.2	−1708.7	−38,564	−31,137	−139,980		13,374	−101,090	108,400
	19	1928.4	−1902.8	−49,881	−39,567	−181,250		9,592.7	−141,720	146,750
	b	2664.4	−2053.3	−58,543	−50,232	−213,380		4,595.2	−174,750	177,090
1	17	999.55	−1530.3	−28,374	−25,249	−105,500	26,023	13,819	−69,424	77,266
	18	744.61	−1444.6	−20,602	−30,848	−121,480		10,885	−85,019	90,952
	19	691.00	−1456.6	−18,154	−38,266	−132,490		7,825.9	−95,423	99,567
	b	427.90	−1376.9	−9,780.7	−46,810	−124,080		4,595.8	−87,861	90,247
2	17	999.45	−1530.3	−28,371	−25,249	−105,500	25,967	12,720	−69,516	77,295
	18	729.23	−1438.5	−20,185	−30,842	−121,070		10,785	−84,702	90,577
	19	691.60	−1456.8	−18,169	−33,248	−132,120		7,727.0	−95,147	99,237
	b	96.000	−1275.5	−2,544.3	−46,680	−116,540		4,595.5	−80,413	82,807
3	17	999.45	−1530.3	−28,371	−25,249	−105,500	25,998	13,782	−69,459	77,277
	18	744.46	−1444.5	−20,598	−30,848	−121,480		10,845	−85,054	90,963
	19	682.10	−1453.3	−17,925	−38,263	−132,260		7,784.7	−95,228	99,349
	b	296.00	−1336.1	−6,904.9	−46,761	−121,010		4,595.4	−84,826	87,215
4	17	999.45	−1530.3	−28,371	−25,249	−105,500	26,008	13,797	−69,445	77,273
	18	734.30	−1440.5	−20,322	−30,844	−121,200		10,865	−84,760	90,682
	19	691.90	−1456.9	−18,177	−38,254	−132,250		7,811.4	−95,204	99,340
	b	397.50	−1366.8	−9,117.9	−46,781	−123,220		4,595.2	−87,022	89,408
5	17	999.45	−1530.3	−28,371	−25,249	−105,500	⁎26,006	13,704	−69,448	77,274
	18	734.33	−1440.5	−20,323	−30,844	−121,200		10,862	−84,763	90,683
	19	691.90	−1456.9	−18,177	−38,254	−132,250		7,807.8	−95,207	99,341
	b	382.00	−1362.1	−8,779.9	−46,777	−122,880		4,595.3	−86,685	89,072

⁎ This value of $\sigma_{t,t}$ is also substituted for the original value of $\sigma_{t,t}$ used in table I(a) to compute plastic stress for stations a to 16.

TABLE II.—ABRIDGED VALUES FROM CALCULATION OF STRESS DISTRIBUTION FOR EXAMPLE II

	1	2	5	6	7	25	25a	25b	38	39	54	60	61
n	r_n	h_n	E_n	α_n	ΔT_n	H'_n	$[P'_n]+[Q'_n]$	$H'_n-[P'_n]-[Q'_n]$	$\sigma_{r,n}$	$\sigma_{t,n}$	$\frac{H'_n-[P'_n]-[Q'_n]}{-P_n}$	$\sigma_{r,n}$	$\sigma_{t,n}$
a	0.5000	4.3750	29.700×10⁵	8.5060×10⁻⁶	130	---	---	---	36,093	36,093	---	35,685	35,685
2	.6250	4.3750	29.700	8.5060	130	0 ×10⁻⁶	0 ×10⁻⁴	0 ×10⁻⁶	36,037	36,069	0 ×10⁻⁴	35,629	35,661
3	.7500	4.3750	29.700	8.5060	130	0	0	0	35,973	36,035	0	35,505	35,627
4	1.0000	4.3750	29.700	8.5060	130	0	0	0	35,814	35,944	0	35,106	35,536
5	1.2500	4.3750	29.700	8.5060	130	0	0	0	35,613	35,821	0	35,205	35,413
6	1.5000	4.3750	29.700	8.5060	130	0	0	0	35,370	35,675	0	34,962	35,267
7	2.0000	4.37f0	29.700	8.5060	130	0	0	0	34,746	35,295	0	34,338	34,887
8	3.0000	3.8400	29.700	8.5060	130	0	0	0	37,240	36,215	0	36,781	35,783
9	4.0000	3.2750	29.700	8.5070	131	8.6400	0	8.6400	39,977	37,557	8.6400	39,451	37,056
10	5.0000	2.6800	29.700	8.5180	138	61.060	0	61.060	43,774	38,228	61.060	43,149	37,700
11	5.5000	2.3720	29.600	8.5330	147	78.870	0	78.870	46,415	37,649	78.870	45,720	37,083
12	6.0000	2.2100	29.600	8.5620	165	158.38	0	158.38	46,390	34,176	158.38	45,667	38,581
13	6.5000	2.1600	20.400	8.6130	197	284.03	0	284.03	43,627	26,320	284.03	42,887	26,710
14	7.0000	2.1550	29.200	8.7000	251	486.94	0	486.94	39,275	12,677	486.94	38,543	12,060
15	7.5000	2.7000	28.700	8.8410	339	813.40	0	813.40	26,535	-12,109	813.40	25,954	-12,673
16	8.0000	2.7000	27.000	9.0680	481	1364.6	0	1364.6	19,876	-47,387	1364.6	19,296	-47,941
17	8.2500	2.5500	27.300	9.2280	579	980.14	20.250	959.89	16,863	-70,310	838.94	16,301	-67,610
18	8.5000	2.3800	26.400	9.4200	700	1252.2	672.87	579.33	13,459	-80,687	390.03	13,031	-78,003
19	8.7500	2.1450	24.700	9.6570	848	1595.1	1236.5	358.60	10,192	-81,665	251.64	9,988	-72,108
b	9.0000	1.9100	20.700	9.9490	1030	2058.3	2282.4	-224.10	7,062	-61,549	-105.13	7,062	-56,196

TABLE III.—ABRIDGED VALUES FROM CALCULATION OF STRESS DISTRIBUTION FOR EXAMPLE III

	1	2	5	6	7	25	25a	25b	38	39	54	60	61
n	r_n	h_n	E_n	α_n	ΔT_n	H'_n	$[P'_n]+[Q'_n]$	$H'_n-[P'_n]-[Q'_n]$	$\sigma_{r,n}$	$\sigma_{t,n}$	$\frac{H'_n-[P'_n]-[Q'_n]}{-P_n}$	$\sigma_{r,n}$	$\sigma_{t,n}$
a	0.5000	4.3750	28.800×10⁶	8.8260×10⁻⁶	330	---	---	---	44,435	44,435	---	44,418	44,418
2	.6250	4.3750	28.800	8.8260	330	0 ×10⁻⁶	0 ×10⁻⁴	0 ×10⁻⁶	44,361	44,403	0 ×10⁻⁴	44,344	44,386
3	.7500	4.3750	28.800	8.8260	330	0	0	0	44,277	44,359	0	44,260	44,342
4	1.0000	4.3750	28.800	8.8260	330	0	0	0	44,066	44,238	0	44,049	44,221
5	1.2500	4.3750	28.800	8.8260	330	0	0	0	43,802	44,079	0	43,785	44,062
6	1.5000	4.3750	28.800	8.8260	330	0	0	0	43,480	43,884	0	43,463	43,867
7	2.0000	4.3750	28.800	8.8260	330	0	0	0	42,655	43,381	0	42,638	43,364
8	3.0000	3.8400	28.800	8.8280	331	9.5000	0	9.5000	45,497	44,159	9.5000	45,478	44,141
9	4.0000	3.2750	28.700	8.8360	336	46.800	0	46.800	48,399	44,631	46.800	48,377	44,642
10	5.0000	2.6800	28.700	8.8620	352	150.50	0	150.50	52,198	43,481	150.50	52,172	43,459
11	5.5000	2.3720	28.600	8.8890	369	160.60	0	160.60	54,778	41,125	160.60	54,749	41,102
12	6.0000	2.2100	28.400	8.9310	395	247.70	0	247.70	54,062	35,558	247.70	54,032	35,533
13	6.5000	2.1600	28.200	8.9960	436	394.60	0	394.60	50,068	25,238	394.60	50,038	25,212
14	7.0000	2.1550	27.900	9.0680	496	587.80	0	587.80	44,243	9,660	587.80	44,212	9,634
15	7.5000	2.7000	27.300	9.2290	581	851.90	0	851.90	29,200	-15,112	851.90	29,176	-15,136
16	8.0000	2.7000	26.400	9.4200	700	1232.0	0	1232.0	21,352	-44,828	1232.0	21,328	-44,851
17	8.2500	2.5500	25.700	9.5400	775	799.50	141.19	658.31	18,041	-58,588	633.34	18,026	-57,981
18	8.5000	2.3800	24.500	9.6790	862	949.80	872.12	77.68	14,659	-56,752	91.355	14,656	-55,825
19	8.7500	2.1450	22.400	9.8410	963	1133.6	1343.5	-209.90	11,807	-44,465	200.34	11,807	-44,478
b	9.0000	1.9100	19.300	10.029	1080	1354.1	2163.4	-809.30	9,339	-21,474	-809.30	9,339	-21,485

TABLE IV.—CALCULATION OF STRESS DISTRIBUTION FOR EXAMPLE IV

(a) Abridged values

	1	2	5	6	7	25	25a	25b	38	39	72	78	79
n	r_n	h_n	E_n	α_n	ΔT_n	H'_n	$[P'_n]+[Q'_n]$	$H'_n-[P'_n]-[Q'_n]$	$\sigma_{r,n}$	$\sigma_{t,n}$	$\frac{H'_n-[P'_n]-[Q'_n]}{-Q_n}$	$\sigma_{r,n}$	$\sigma_{t,n}$
a	0.5000	4.3750	27.600×10⁶	9.1470×10⁻⁶	530	0 ×10⁻⁴	0 ×10⁻⁴	---	46,006	46,006	---	46,005	46,005
2	.6250	4.3750	27.600	9.1470	530	0	0	0 ×10⁻⁶	45,932	45,974	0 ×10⁻⁶	45,931	45,973
3	.7500	4.3750	27.600	9.1470	530	0	0	0	45,848	45,930	0	45,847	45,929
4	1.0000	4.3750	27.600	9.1470	530	0	0	0	45,637	45,809	0	45,636	45,808
5	1.2500	4.3750	27.600	9.1470	530	0	0	0	45,373	45,650	0	45,372	45,649
6	1.5000	4.3750	27.600	9.1470	530	0	0	0	45,051	45,455	0	45,050	45,454
7	2.0000	4.3750	27.600	9.1490	531	10.200	0	10.200	44,194	44,698	10.200	44,193	44,697
8	3.0000	3.8400	27.600	9.1590	537	59.700	0	59.700	46,959	44,419	59.700	46,958	44,418
9	4.0000	3.2750	27.500	9.1840	553	161.00	0	161.00	49,149	42,507	161.00	49,448	42,506
10	5.0000	2.6800	27.300	9.2380	587	343.90	0	343.90	52,329	37,155	343.90	52,328	37,154
11	5.5000	2.3720	27.100	9.2820	614	276.40	0	276.40	54,197	32,527	276.40	54,195	32,526
12	6.0000	2.2100	26.800	9.3380	649	361.30	0	361.30	52,668	25,030	361.30	52,666	25,028
13	6.5000	2.1600	26.500	9.4080	693	459.30	0	459.30	47,920	14,400	459.30	47,918	14,399
14	7.0000	2.1550	25.900	9.5000	750	605.30	0	605.30	41,517	227	605.30	41,515	227
15	7.5000	2.7000	25.100	9.6100	819	745.60	0	745.60	26,780	-19,203	745.60	26,778	-19,204
16	8.0000	2.7000	23.800	9.7480	905	951.30	0	951.30	19,146	-36,527	951.30	19,145	-36,528
17	8.2500	2.5500	22.700	9.9870	954	705.70	166.17	539.53	16,107	-45,462	538.54	16,105	-45,443
18	8.5000	2.3800	21.200	9.9120	1007	453.80	858.44	-404.64	13,200	-32,446	-405.17	13,199	-32,415
19	8.7500	2.1450	19.800	10.007	1066	685.60	1334.0	-648.40	11,002	-16,554	-647.94	11,003	-16,536
b	9.0000	1.9100	17.900	10.109	1130	756.00	2163.4	-1407.4	9,340	10,470	-1406.5	9,334	10,470

TABLE IV.—CALCULATION OF STRESS DISTRIBUTION FOR EXAMPLE IV—Concluded

(b) Calculation of effect of creep on final stresses

n	63 c_n	64 Γ_n, (63)×5	65 $\frac{\delta_{r,n}}{(41)\times2}\times$ (64) $[2\times(38)-(39)]$	66 $\frac{\delta_{t,n}}{(41)\times2}\times$ (64) $[2\times(39)-(38)]$	67 (65)×(42)	68 (65)$_{n-1}$×(43)	69 (66)×(44)	70 (66)$_{n-1}$×(45)	71 (67)+(68)− (69)+(70)
17	0.2×10⁻⁴	1.0×10⁻⁴	0.70226×10⁻⁴	−0.96766×10⁻⁴	0.010641×10⁻⁴	0.00000×10⁻⁴	−0.98237×10⁻⁴	0.00000×10⁻⁴	0.99301×10⁻⁴
18	.3	1.5	1.0848	−1.4396	.015953	.010641	−1.4608	−.95300	.53439
19	.2	1.0	.80246	−.91800	.011464	.015953	−.93113	−1.4184	−.45985
b	0	0	0	0	0	.011464	0	−.90488	−.89342

n	72 $H'_n-[P'_n]-[Q'_n]$ $-Q'_n$ (25b)−(71)	73 M_n, [(72)×(10)+(14)× (21)]+(26)	74 M'_n, [(73)×(8)+(14)× (20)]+(26)	75 $B_{r,n}$, (27)×(75)$_{n-1}$+ (28)×(76)$_{n-1}$+ (73)	76 $B_{t,n}$, (29)×(75)$_{n-1}$+ (30)×(76)$_{n-1}$+ (74)	77 $\sigma_{t,n}$, $[\sigma_{r,t}-(75)_b]+$ (33) $_b$	78 $\sigma_{r,n}$, (33)×(77)+(75)	79 $\sigma_{t,n}$, (34)×(77)+(76)
17	538.54×10⁻⁴	−2469.1	−12,876	−52,373	−106,190	46,005	16,105	−45,443
18	−405.17	−2247.2	7,607.5	−59,831	−91,828	------	13,199	−32,418
19	−647.94	−2306.2	11,751	−69,530	−76,973	------	11,003	−16,536
b	−1406.5	−2230.7	23,905	−80,379	−50,985	------	9,334	10,470

TABLE V.—ABRIDGED VALUES FROM CALCULATION OF STRESS DISTRIBUTION FOR EXAMPLE V

n	1 r_n	2 k_n	5 E_n	6 α_n	7 ΔT_n	25 H'_n	25a $[P'_n]+[Q'_n]$	25b $H'_n-[P'_n]-[Q'_n]$	38 $\sigma_{r,n}$	39 $\sigma_{t,n}$	54 $H'_n-[P'_n]-[Q'_n]$ $-P'_n$	60 $\sigma_{r,n}$	61 $\sigma_{t,n}$
a	0.5000	4.3750	28.800×10⁶	8.8250×10⁻⁶	331	------	------	------	22,285	22,285	------	22,285	22,285
2	.6250	4.3750	28.800	8.8300	332	9.49×10⁻⁴	0 ×10⁻⁴	9.49 ×10⁻⁴	22,253	22,023	9.49×10⁻⁴	22,253	22,023
3	.7500	4.3750	28.800	8.8310	333	9.16	0	9.16	22,181	21,811	9.16	22,181	21,811
4	1.0000	4.3750	28.800	8.8330	334	9.50	0	9.50	22,027	21,645	9.50	22,027	21,645
5	1.2500	4.3750	28.700	8.8390	338	37.36	0	37.36	21,801	20,687	37.36	21,801	20,687
6	1.5000	4.3750	28.700	8.8440	341	28.22	0	28.22	21,501	20,085	28.22	21,501	20,085
7	2.0000	4.3750	28.700	8.8580	350	84.50	0	84.50	20,744	18,160	84.50	20,744	18,160
8	3.0000	3.8400	28.500	8.8970	374	226.70	0	226.70	21,090	14,149	226.70	21,090	14,149
9	4.0000	3.2750	28.300	8.9530	409	334.78	0	334.78	20,964	8,300	334.78	20,964	8,300
10	5.0000	2.6800	28.100	9.0240	453	426.09	0	426.09	20,680	1,010	426.09	20,680	1,010
11	5.5000	2.3720	28.000	9.0650	479	254.27	0	254.27	20,585	−3,342	254.27	20,585	−3,342
12	6.0000	2.2100	27.800	9.1120	508	287.76	0	287.76	19,144	−8,724	287.76	19,144	−8,724
13	6.5000	2.1600	27.600	9.1620	539	309.42	0	309.42	16,529	−14,887	309.42	16,529	−14,887
14	7.0000	2.1550	27.400	9.2140	572	332.09	0	332.09	13,400	−21,552	332.09	13,400	−21,552
15	7.5000	2.7000	27.100	9.2720	608	366.97	0	366.97	7,748	−29,867	366.97	7,748	−29,867
16	8.0000	2.7000	26.800	9.3330	646	391.74	0	391.74	4,365	−37,781	391.74	4,365	−37,781
17	8.2500	2.5500	26.700	9.3650	666	207.97	167.16	40.840	2,879	−37,429	40.840	2,879	−37,429
18	8.5000	2.3800	26.500	9.3990	687	220.02	858.97	−638.97	1,675	−19,393	−638.97	1,675	−19,393
19	8.7500	2.1450	26.300	9.4490	708	232.78	1333.5	−1100.5	1,171	9,833	−1100.5	1,171	9,833
b	9.0000	1.9100	26.100	9.4990	730	244.38	2162.5	−1918.5	1,764	58,858	−1918.5	1,764	58,858

TABLE VI.—ABRIDGED VALUES FROM CALCULATION OF STRESS DISTRIBUTION FOR EXAMPLE VI

n	1 r_n	2 k_n	5 E_n	6 α_n	7 ΔT_n	25 H'_n	25a $[P'_n]+[Q'_n]$	25b $H'_n-[P'_n]-[Q'_n]$	38 $\sigma_{r,n}$	39 $\sigma_{t,n}$	54 $H'_n-[P'_n]-[Q'_n]$ $-P'_n$	60 $\sigma_{r,n}$	61 $\sigma_{t,n}$
a	0.5000	4.3750	29.300×10⁶	8.6760×10⁻⁶	236	------	------	------	3616	3,616	------	3750	3,750
2	.6250	4.3750	29.300	8.6770	237	8.91×10⁻⁴	0 ×10⁻⁴	8.91×10⁻⁴	3592	3,375	8.91×10⁻⁴	3726	3,509
3	.7500	4.3750	29.300	8.6790	238	9.15	0	9.15	3537	3,160	9.15	3672	3,294
4	1.0000	4.3750	29.300	8.6840	241	27.20	0	27.20	3364	2,529	27.20	3498	2,662
5	1.2500	4.3750	29.200	8.6880	244	27.03	0	27.03	3140	1,956	27.03	3274	2,090
6	1.5000	4.3750	29.200	8.6930	247	27.30	0	27.30	2897	1,402	27.30	3030	1,536
7	2.0000	4.3750	29.200	8.7010	252	45.48	0	45.48	2417	557	45.48	2551	690
8	3.0000	3.8400	29.100	8.7190	263	100.44	0	100.44	1725	−1,301	100.44	1876	−1,160
9	4.0000	3.2750	29.100	8.7370	274	100.84	0	100.84	933	−3,144	100.84	1106	−2,990
10	5.0000	2.6800	29.000	8.7560	286	110.28	0	110.28	2	−5,260	110.28	207	−5,087
11	5.5000	2.3720	29.000	8.7640	291	46.11	0	46.11	−545	−6,093	46.11	−317	−5,907
12	6.0000	2.2100	28.900	8.7730	297	55.26	0	55.26	−1108	−7,185	55.26	−868	−6,991
13	6.5000	2.1600	28.900	8.7820	302	46.58	0	46.58	−1639	−8,043	46.58	−1396	−7,843
14	7.0000	2.1550	28.900	8.7910	308	55.46	0	55.46	−2140	−9,150	55.46	−1900	−8,947
15	7.5000	2.7000	28.900	8.7990	313	46.46	0	46.46	−2165	−9,819	46.46	−1974	−9,631
16	8.0000	2.7000	28.800	8.8090	319	55.98	0	55.98	−2676	−10,889	55.98	−2466	−10,702
17	8.2500	2.5500	28.800	8.8140	322	28.04	167.16	−139.12	−3025	−6,756	−139.12	−2824	−6,564
18	8.5000	2.3900	28.800	8.8170	324	18.60	858.97	−840.37	−3000	17,132	−840.37	−2785	17,329
19	8.7500	2.1450	28.900	8.8220	327	28.09	1333.5	−1305.4	−2197	53,534	−1305.4	−1959	53,740
b	9.0000	1.9100	28.800	8.8260	330	27.79	2162.5	−2134.7	0	112,600	−1461.0	0	93,672

TABLE VII.—ABRIDGED VALUES FROM CALCULATION OF STRESS DISTRIBUTION FOR EXAMPLE VII

	1	2	5	6	7	25	25a	25b	38	39	54	60	61
n	r_n	h_n	E_n	α_n	ΔT_n	H'_n	$[P'_n]+[Q'_n]$	$H'_n-[P'_n]-[Q'_n]$	$\sigma_{r,n}$	$\sigma_{t,n}$	$H'_n-[P'_n]-[Q'_n]-P'_n$	$\sigma_{r,n}$	$\sigma_{t,n}$
a__	0.5000	4.3750					0 ×10⁻⁶	0 ×10⁻⁴	−2468	−2,468	0 ×10⁻⁶	−2356	−2,356
2__	.6250	4.3750					0	0	−2468	−2,408	0	−2356	−2,356
3__	.7500	4.3750					0	0	−2468	−2,468	0	−2356	−2,356
4__	1.0000	4.3750					0	0	−2468	−2,468	0	−2356	−2,356
5__	1.2500	4.3750					0	0	−2468	−2,468	0	−2356	−2,356
6__	1.5000	4.3750	Constant at 30.000×10⁶	Constant at 8.2970×10⁻⁶	Constant at 0	Constant at 0	0	0	−2468	−2,468	0	−2356	−2,356
7__	2.0000	4.3750					0	0	−2468	−2,468	0	−2356	−2,356
8__	3.0000	3.8400					0	0	−2779	−2,614	0	−2653	−2,400
9__	4.0000	3.2750					0	0	−3183	−2,849	0	−3039	−2,720
10_	5.0000	2.6800					0	0	−3779	−3,193	0	−3608	−3,049
11_	5.5000	2.3720					0	0	−4202	−3,428	0	−4012	−3,273
12_	6.0000	2.2100					0	0	−4437	−3,604	0	−4237	−3,442
13_	6.5000	2.1600					0	0	−4475	−3,705	0	−4273	−3,537
14_	7.0000	2.1550					0	0	−4432	−3,762	0	−4232	−3,592
15_	7.5000	2.7000					0	0	−3518	−3,476	0	−3359	−3,319
16_	8.0000	2.7000					0	0	−3515	−3,479	0	−3356	−3,321
17_	8.2500	2.5500					167.16	−167.16	−3544	1,353	−167.16	−3476	1,519
18_	8.5000	2.3800					858.97	−858.97	−3378	26,512	−858.97	−3199	26,677
19_	8.7500	2.1450					1333.5	−1333.5	−2292	65,023	−1333.5	−2093	65,195
b__	9.0000	1.9100					1488.8	−1488.8	0	107,180	−947.81	0	91,109

TABLE VIII.—CALCULATION OF STRESS DISTRIBUTION FOR PARALLEL-SIDED DISK

(a) Abridged values

	1	2	5	6	7	25	25a	25b	38	39	40	41	60	61
n	r_n	h_n	E_n	α_n	ΔT_n	H'_n	$[P'_n]+[Q'_n]$	$H'_n-[P'_n]-[Q'_n]$	$\sigma_{r,n}$	$\sigma_{t,n}$	$\sigma_{p,n}$	$\sigma_{s,n}$	$\sigma_{r,n}$	$\sigma_{t,n}$
a__	0.5000								0	176,040		176,040	0	124,520
2__	.6250								31,650	142,520		129,620	24,062	127,150
3__	.7500								48,400	124,850		109,030	41,519	124,510
4__	1.0000								64,573	106,350		92,872	60,031	111,630
5__	1.5000								74,394	91,900		84,518	72,549	93,977
6__	2.0000	Constant at 1.0000	Constant at 30.000×10⁶	Constant at 8.2970×10⁻⁶	Constant at 0	Constant at 0	Constant at 0	Constant at 0	75,607	86,673	Constant at 100,000	81,704	74,625	87,813
7__	2.5000								74,187	83,268		79,119	73,589	84,005
8__	3.0000								71,369	80,278		76,215	70,976	80,803
9__	3.5000								67,553	77,268		72,898	67,282	77,669
10_	4.0000								62,892	74,060		69,156	62,700	74,390
11_	4.5000								57,471	70,579		65,024	57,332	70,845
12_	5.0000								51,322	66,782		60,551	51,223	67,009
13_	5.5000								44,473	62,650		55,827	44,401	62,847
14_	6.0000								36,934	58,163		50,979	36,883	58,339
15_	6.5000								28,711	53,317		46,219	28,678	53,470
16_	7.0000								19,813	48,103		41,573	19,792	48,249
17_	7.5000								10,248	42,518		38,433	10,232	42,654
b__	8.0000								0	36,562		36,562	0	36,919

(b) Calculation for first approximation of plastic-stress distribution

	42	43	44	45	46	46a	47	48	49	50	51	52	53
n	$(9)/(1)$	$(9)/(1)_{n-1}$	$1+(42)$	$1-(43)$	$\epsilon_{p,n}$ (graph reading, fig. 7)	$\epsilon_{p,n}$ (estimate)	$\Delta_{r,n}$ $\frac{(46a)}{(41)\times2}\times$ $[2\times(38)-(39)]$	$\Delta_{t,n}$ $\frac{(46a)}{(41)\times2}\times$ $[2\times(39)-(38)]$	$(47)\times(42)$	$(47)_{n-1}\times(43)$	$(48)\times(44)$	$(48)_{n-1}\times(45)$	P'_n $(49)+(50)-(51)+(52)$
a__					1800×10⁻⁶	1800×10⁻⁴	−900.00×10⁻⁶	1800.00×10⁻⁴					
2__	0.10000	0.12500	1.1000	0.87500	550	550	−168.06	587.56	−16.806×10⁻⁶	−112.50×10⁻⁴	591.32×10⁻⁶	1575.0×10⁻⁴	854.37×10⁻⁴
3__	.08333	.10000	1.0833	.90000	300	300	−38.59	276.95	−3.2158	−16.806	300.02	483.80	163.75
4__	.12500	.16670	1.1250	.83333	0	0	0	0		−6.4330	0	230.78	224.34

	54	55	56	57	58	59	60	61	62
n	$H'_n-[P'_n]-[Q'_n]-P'_n$ $(25b)-(53)$	M_n $[(54)\times(10)+(14)\times(21)]+(26)$	M'_n $[(54)\times(8)+(14)\times(20)]+(26)$	$B_{r,n}$ $(27)\times(57)_{n-1}+(28)\times(58)_{n-1}+(55)$	$B_{t,n}$ $(29)\times(57)_{n-1}+(30)\times(58)_{n-1}+(56)$	$[\sigma_{r,n}-(57)_n]+(33)_n$	$\sigma_{r,n}$ $(33)\times(59)+(57)$	$\sigma_{t,n}$ $(34)\times(59)+(58)$	$\sigma_{s,n}$ $\sqrt{\frac{(60)^2+(61)^2}{-(60)\times(61)}}$
a__							0	138,510	138,510
2__	−854.37×10⁻⁴	2,144.1	23,499	2,144.1	23,499		27,216	135,700	124,390
3__	−163.75	117.81	4,475.8	5,589.1	24,590		43,981	122,980	107,030
4__	−224.34	101.23	5,829.7	9,835.0	25,875		61,477	109,960	95,450
5__	0	−1,872.7	−795.28	12,435	19,838				
6__	0	−2,641.2	−1,050.8	11,424	17,021				
7__	0	−3,423.3	−1,302.6	9,013.8	14,655				
8__	0	−4,212.0	−1,551.8	5,667.5	12,209				
9__	0	−5,005.0	−1,799.2	1,533.5	9,519.1	Constant at 138,510			
10_	0	−5,800.2	−2,045.1	−3,328.3	6,519.0				
11_	0	−6,597.3	−2,290.8	−8,889.8	3,178.3				
12_	0	−7,395.5	−2,534.7	−15,136	−518.0				
13_	0	−8,194.6	−2,778.5	−22,060	−4,578.8				
14_	0	−8,994.4	−3,021.9	−29,657	−9,009.6				
15_	0	−9,794.6	−3,265.0	−37,923	−13,814				
16_	0	−10,595	−3,507.8	−46,856	−18,994				
17_	0	−11,396	−3,750.1	−56,454	−24,550				
b__	0	−12,197	−3,992.5	−66,717	−30,483				